FUNDAMENTAL PHYSICS WITH LARGE/MEDIUM/SMALL SCALE STRUCTURES

LECTURE 4

Matteo Viel - SISSA
2022 Winter School
Tenerife (Spain)

Euclid Flagship Simulation

SISSA

PLAN

INTRO

FUNDAMENTAL PHYSICAL TESTS "BEFORE" GALAXIES ARE FORMED IN THE POST-REIONIZATION UNIVERSE

INTENSITY MAPPING
IGM

GALAXY CLUSTERING: DYNAMICAL AND GEOMETRICAL PROBE

WEAK LENSING

GALAXY CLUSTERS

CONNECTIONS

FABIO FINELLI: CMB x LSS

KFIR BLUM: SMALLER SCALES PROPERTIES OF GALAXIES

LUCA AMENDOLA: MODIFICATION OF GRAVITY/DARK ENERGY

OLGA MENA: NEUTRINOS

TRACY SLATYER: DARK MATTER

WEAK (and partly STRONG) LENSING

Hoekstra & Jain 2008
Schneider lectures https://arxiv.org/abs/astro-ph/0509252
Wong et al. 2019 - HoliCow time delays results
Birrer+22
Treu+21 2210.10833 mini review
Martin Crocce [talk]
Martin White lectures
Hoekstra [talk]
Heymans+21 [Kids-1000] LCDM
Trost+21 [Kids-1000] beyond LCDM
Mantz+21 cosmology with gas fraction in Galaxy Clusters
Esposito+22
Costanzi+18
DES 3yr results papers https://www.darkenergysurvey.org/des-year-3-cosmology-results-papers/

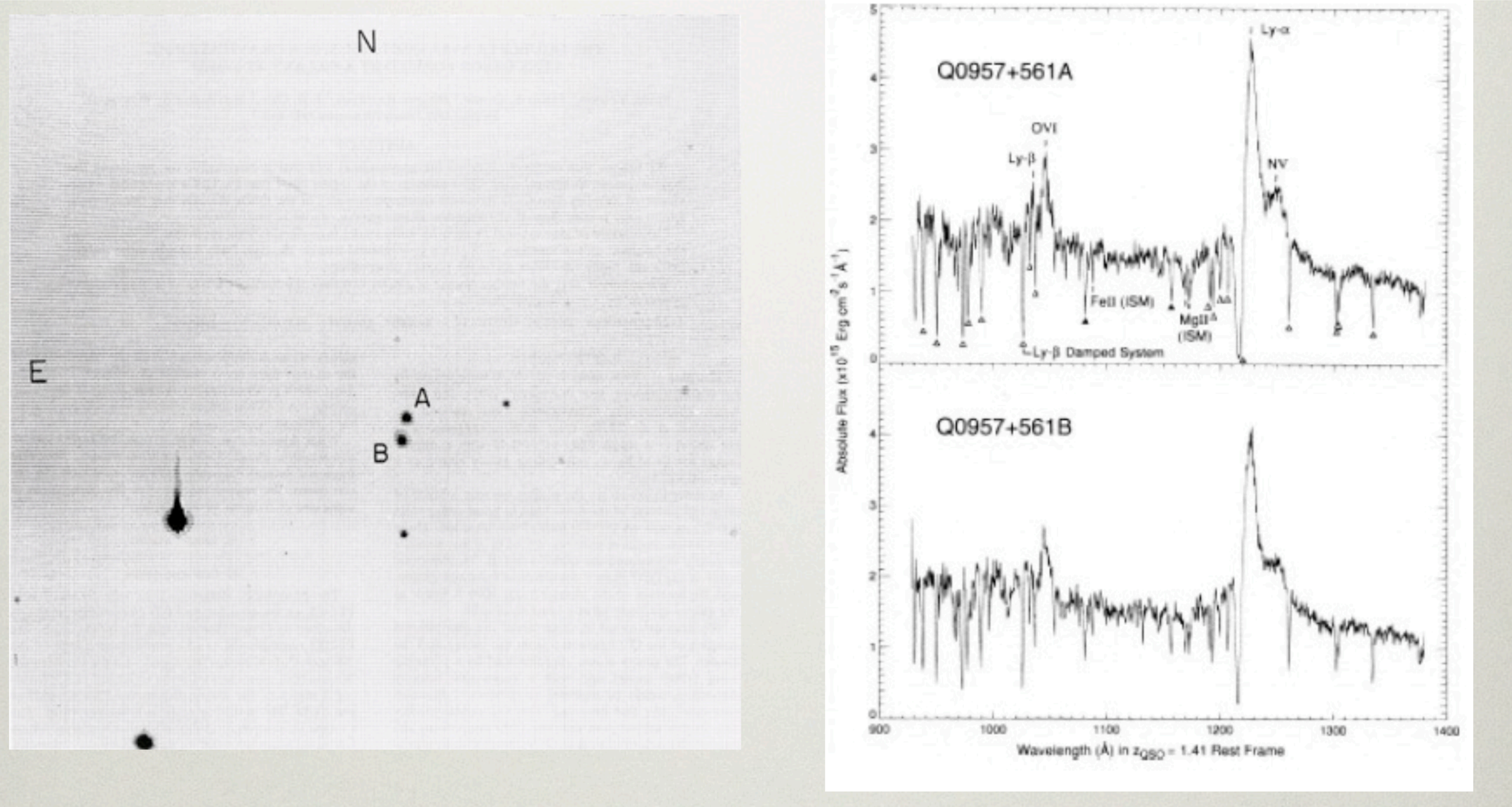

First lensed Quasar Q0957+561A - Welsh (1979)

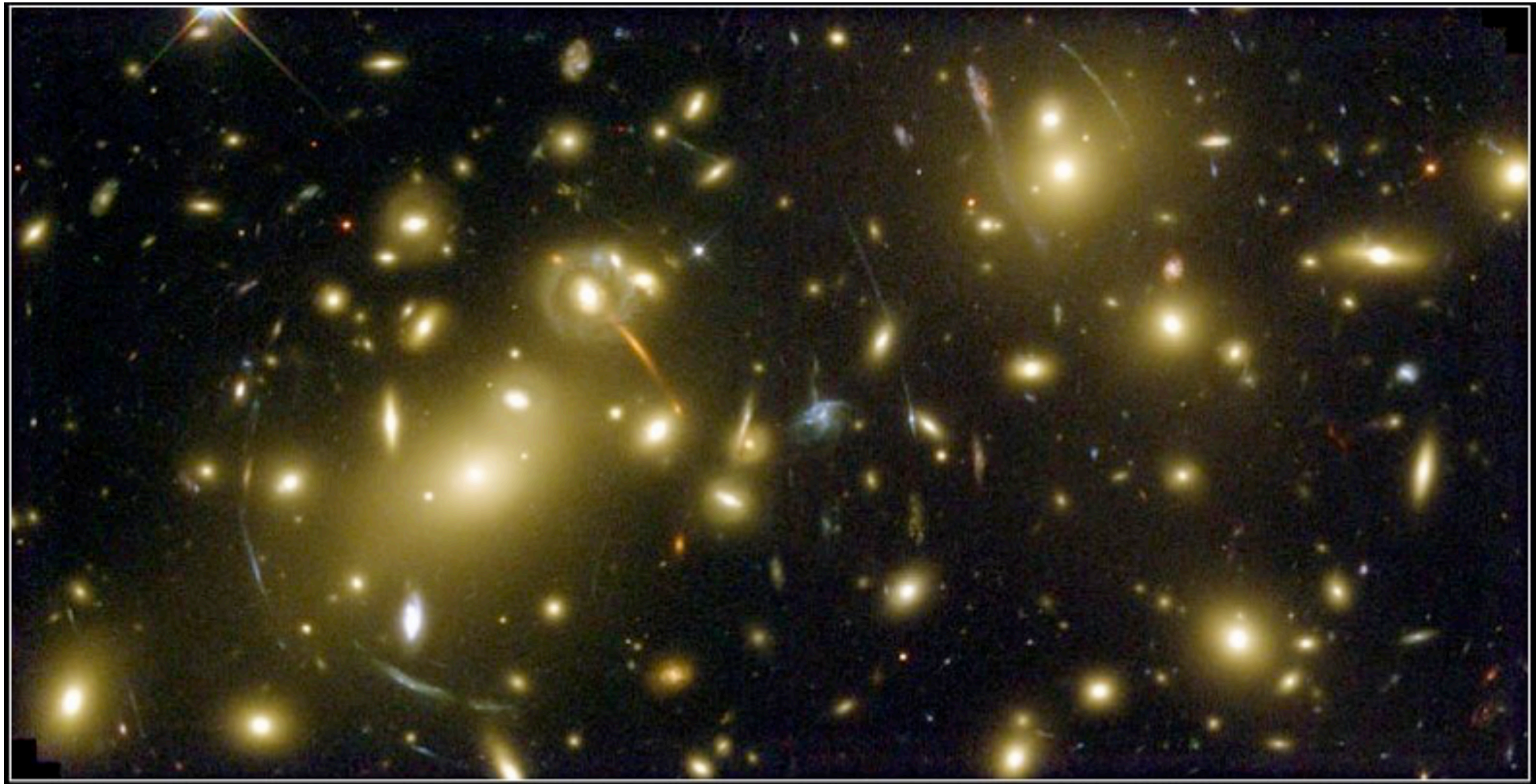

Galaxy Cluster Abell 2218 **HST • WFPC2**

NASA, A. Fruchter and the ERO Team (STScI, ST-ECF) • STScI-PRC00-08

SMACS 0723, known as Webb's First Deep Field

11/07/22

Weak Lensing Basics - I

Assumptions:
1) Gravitational field is weak
2) Deflection angles are small
3) Deflection happens at scales << scale of the Universe

$$d\tau^2 = (c^2 + 2\Phi)dt^2 - (1 - 2\Phi / c^2)ds^2$$

Use GR with line element and Phi Newtonian potential

Use Fermat principle dtau=0

$$dt = \sqrt{\frac{1 - 2\Phi / c^2}{c^2 + 2\Phi}} ds \approx \frac{1}{c}\left(1 - 2\frac{\Phi}{c^2}\right) ds = \frac{n}{c} ds$$

n>1 is an index of refraction
produced by the Newtoniana potential

Weak Lensing Basics - II

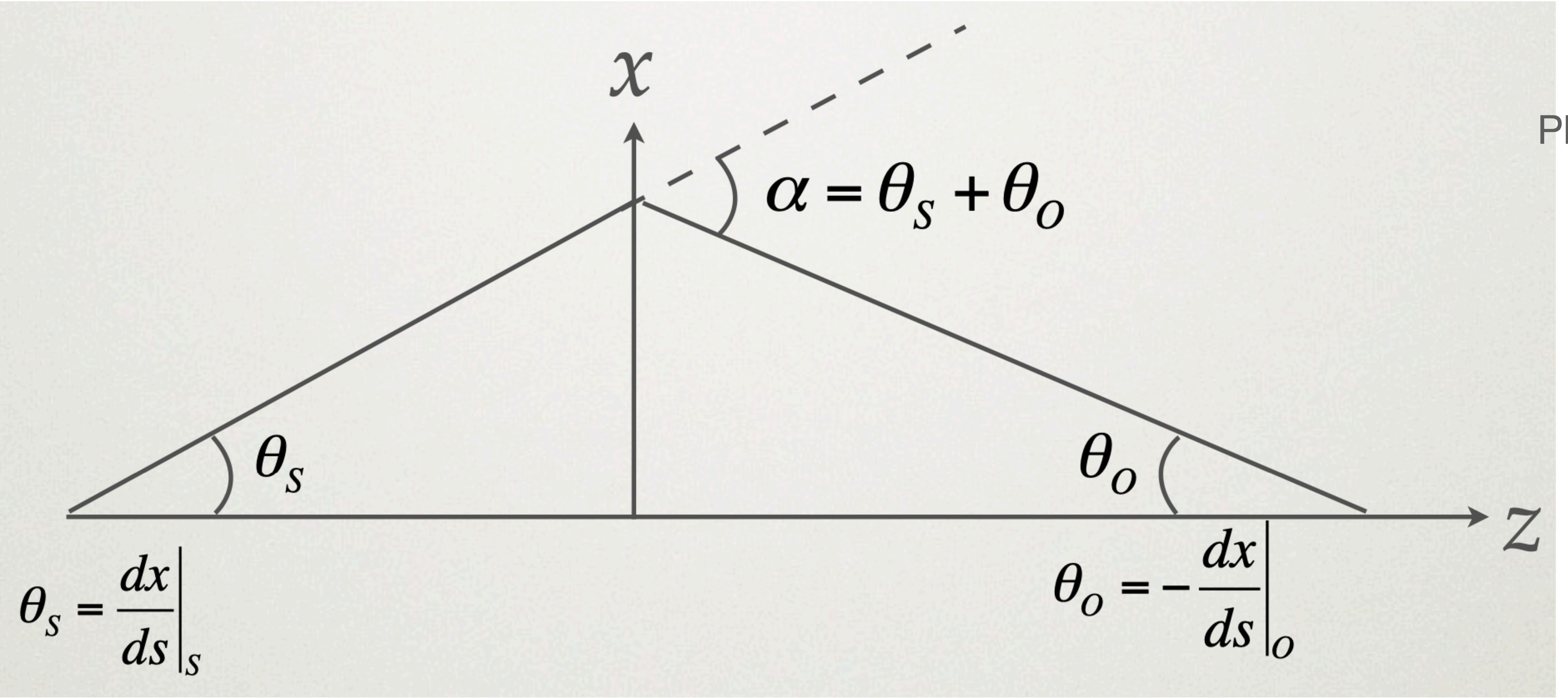

Photons will follow a Path for which the light travel time is stationary to small changes in the path

$$t = \frac{1}{c}\int n \cdot ds$$

$$\vec{\alpha} = \int_S^O ds \vec{\nabla}_\perp n = -\frac{2}{c^2}\int_S^O ds \vec{\nabla}_\perp \Phi$$

$$\Phi(\vec{x}) = -G\int d^3x' \frac{\rho(\vec{x}')}{|\vec{x} - \vec{x}'|}$$

$$\alpha(\vec{x}) = -\frac{4G}{c^2}\vec{\nabla}\int d^2\vec{x}'\Sigma(\vec{x}')\ln|\vec{x} - \vec{x}'|$$

Weak Lensing Basics - III

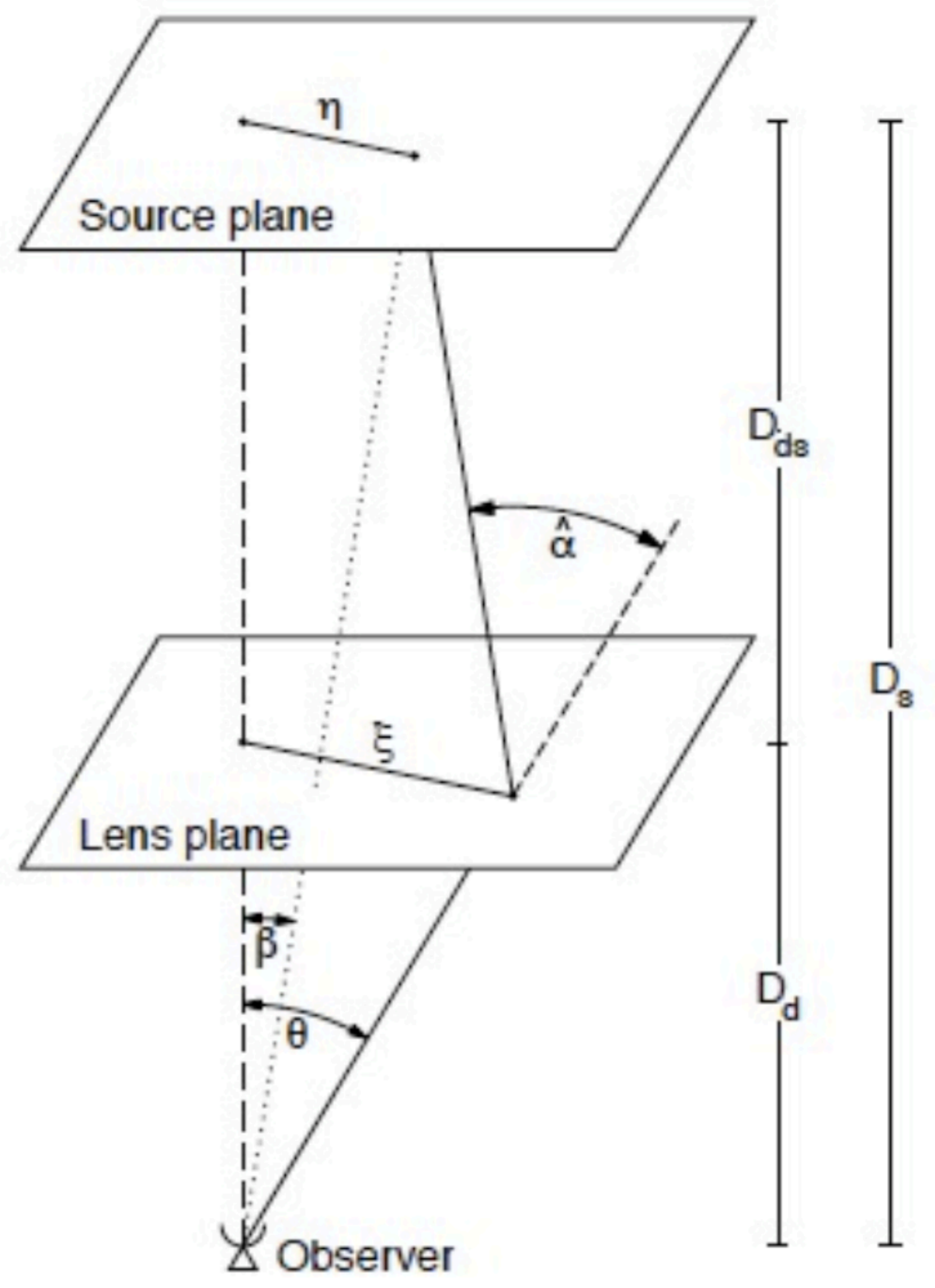

The lens equation

$$\boldsymbol{\eta} = \frac{D_s}{D_d}\boldsymbol{\xi} - D_{ds}\hat{\boldsymbol{\alpha}}(\boldsymbol{\xi})$$

$$\boldsymbol{\eta} = D_s\boldsymbol{\beta} \;\; \text{and} \;\; \boldsymbol{\xi} = D_d\boldsymbol{\theta}$$

$$\boldsymbol{\beta} = \boldsymbol{\theta} - \frac{D_{ds}}{D_s}\hat{\boldsymbol{\alpha}}(D_d\boldsymbol{\theta}) \equiv \boldsymbol{\theta} - \boldsymbol{\alpha}(\boldsymbol{\theta})$$

$$\boldsymbol{\beta} = \boldsymbol{\theta} - \boldsymbol{\alpha}(\boldsymbol{\theta})$$

The mapping from image to source plane is easy.

This is not the case for the mapping from source to image plane:

A source with true position will be observed at all positions that satisfy the lens equation.

Multiple solutions are possible: a single source can be observed at several positions on the sky

... and this is used to measure H0 from time delays! :-)

Weak Lensing Basics - IV

Redshift of sources has to be known: spectroscopy too expensive
photometry is good

$$\kappa(\theta) = \frac{\Sigma}{\Sigma_{crit}}, \qquad \Sigma_{crit} \equiv \frac{c^2}{4\pi G}\frac{D_s}{D_{ls}D_l}$$

convergence

$$\alpha(\theta) = \frac{1}{\pi}\int d^2\vartheta \cdot \kappa(\vartheta)\frac{\theta - \vartheta}{|\theta - \vartheta|^2} \equiv \vec{\nabla}\Psi(\theta)$$

deflection
angle

$$\Psi(\theta) = \frac{1}{\pi}\int d^2\vartheta \cdot \kappa(\vartheta)\ln|\theta - \vartheta|$$

gravitational
potential

$$\nabla^2\Psi(\theta) = 2\kappa(\theta)$$

Poisson-like
equation

Observable effects:

Delays
Deflection
Distortion

Time delays - I

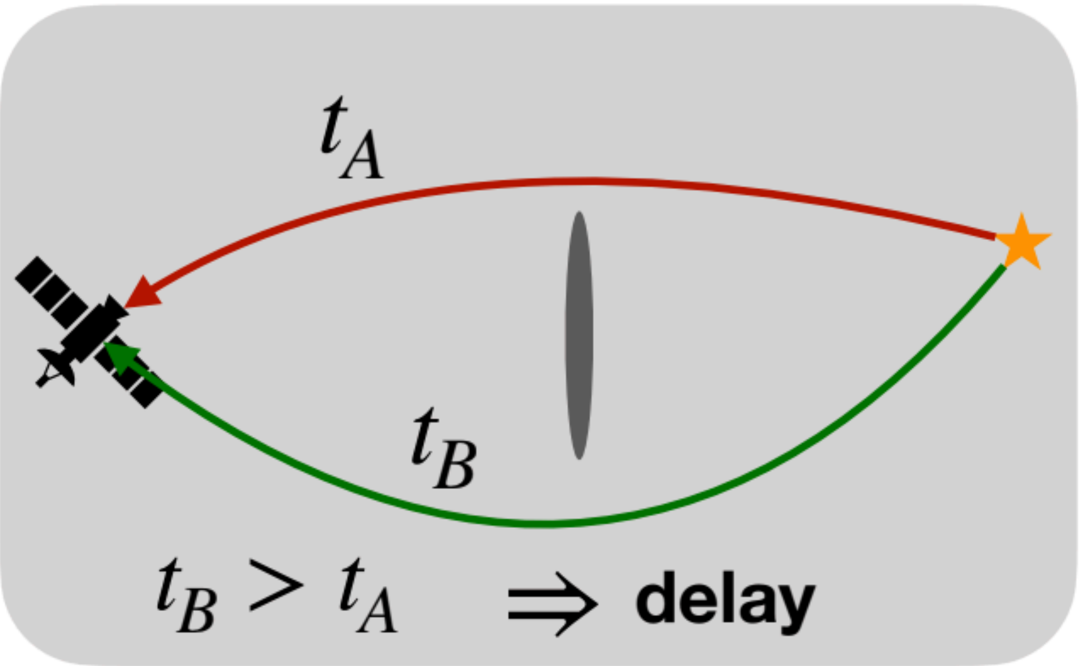

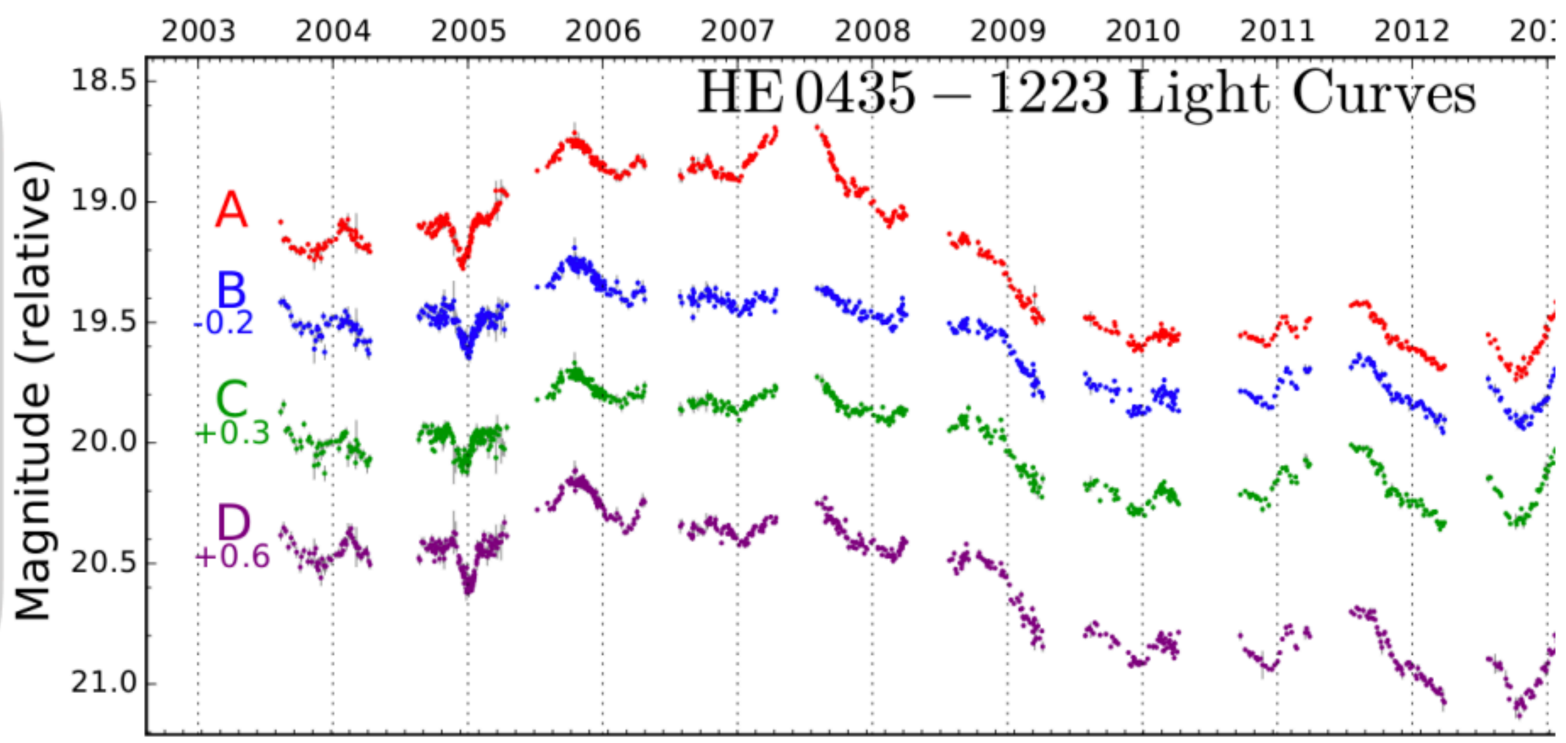

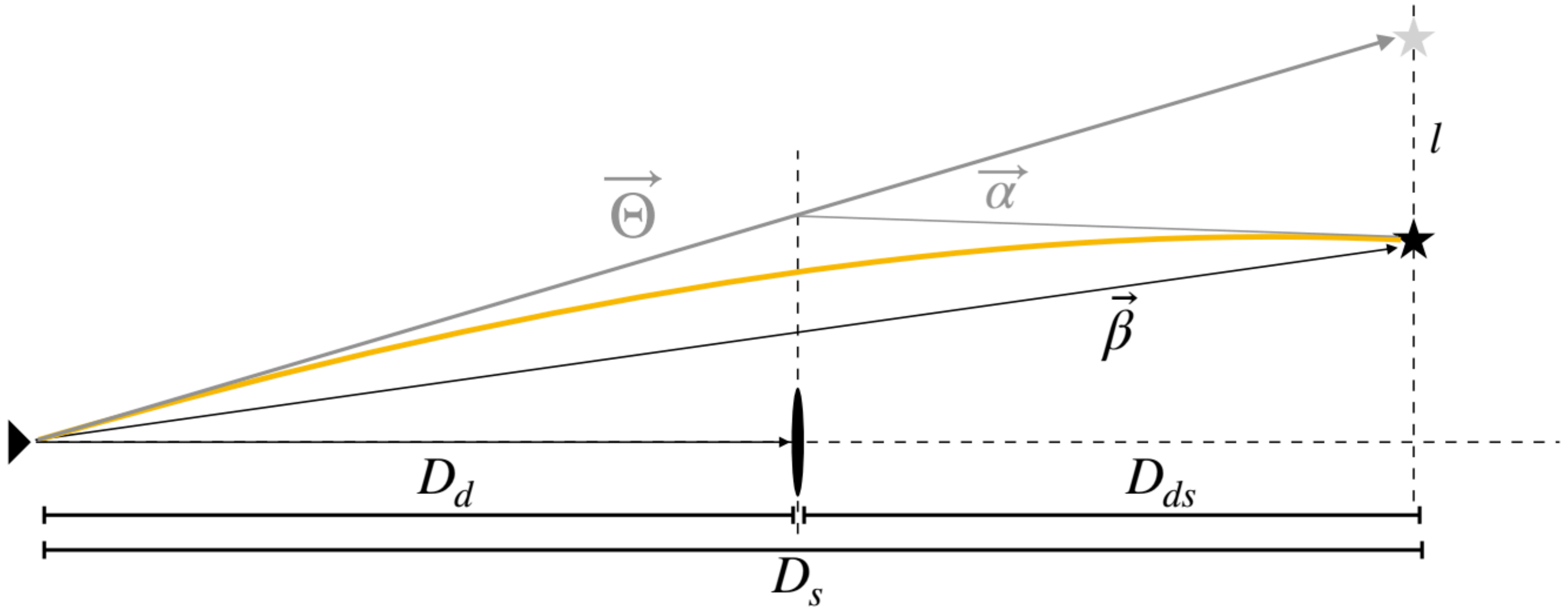

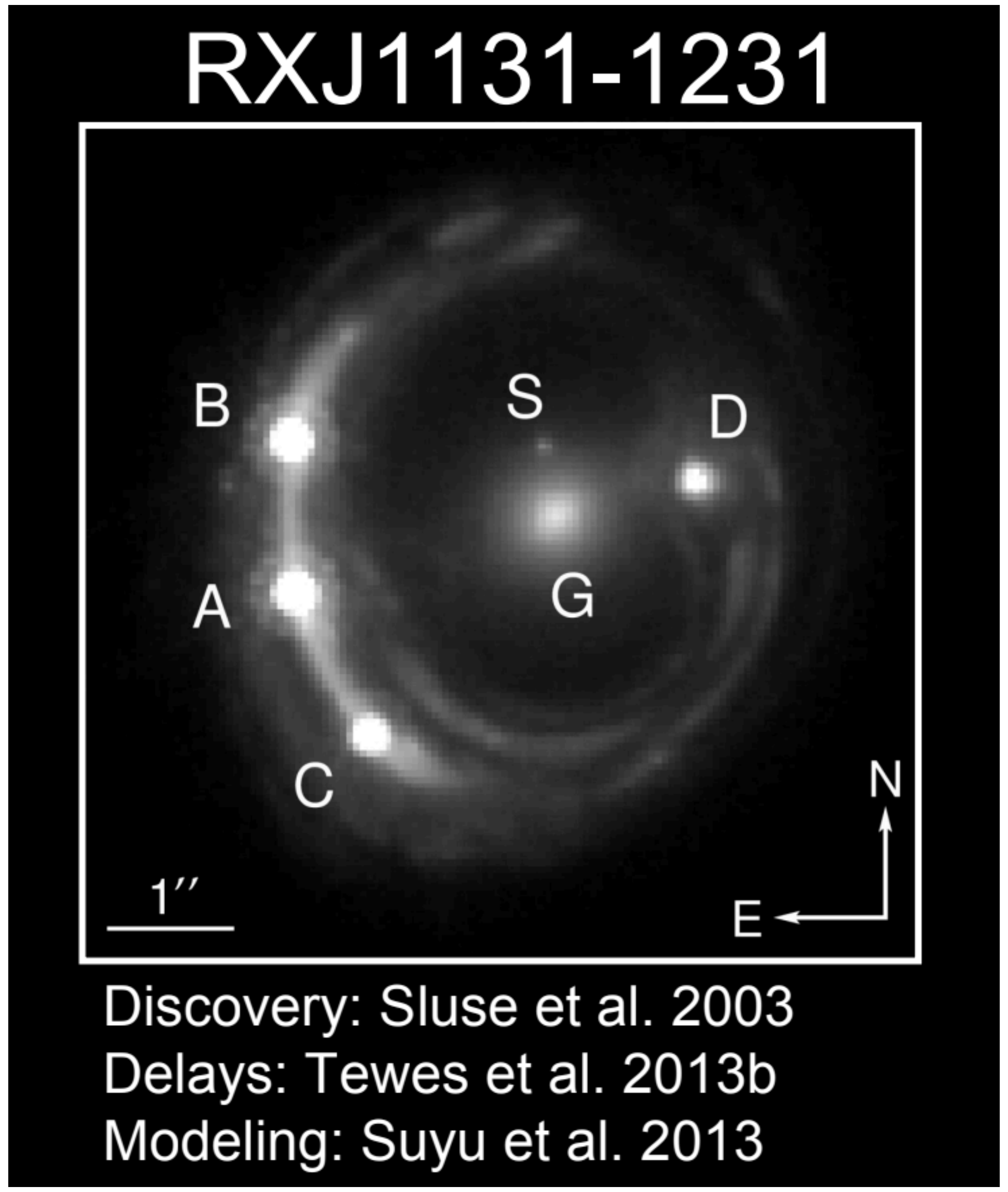

- Generically, taking into account GR and 3-dim

$$t(\vec{\Theta}) = \frac{D_{\Delta t}}{c} \cdot \Phi(\vec{\Theta}, \vec{\beta})$$

Fermat potential

where $\Phi = \frac{1}{2}(\vec{\Theta} - \vec{\beta})^2 - \psi(\vec{\Theta})$ and $D_{\Delta t} \equiv (1 + z_d)\frac{D_d D_s}{D_{ds}}$

geometric

Shapiro delay

Lens potential

Units: (angle)^2/H0

Time delays - II

- The time delay between two paths is then

$$\Delta t_{AB} = \frac{D_{\Delta t}}{c} \cdot \Delta\Phi_{AB}$$

- $D_{\Delta t} = (1+z_d)\frac{D_d D_s}{D_{ds}}$. D's are angular-diameter distances

$$\Rightarrow D_{\Delta t} \propto H_0^{-1}$$

! Problem:

If $\Sigma(\Theta)$ provides a good fit to the data, also

$$\vec{\beta}_\lambda = \lambda\vec{\beta} \quad \text{and} \quad \Sigma'_\lambda(\Theta) \equiv (1-\lambda) + \lambda\Sigma(\Theta)$$

"uniform mass sheet"

mass sheet transformation *(Falco et al. 1987)*

provides an equally good fit (→**degeneracy**).

This affects the prediction of D_{ds} is such a way that

$$H'_{0\lambda} = \lambda H_0$$

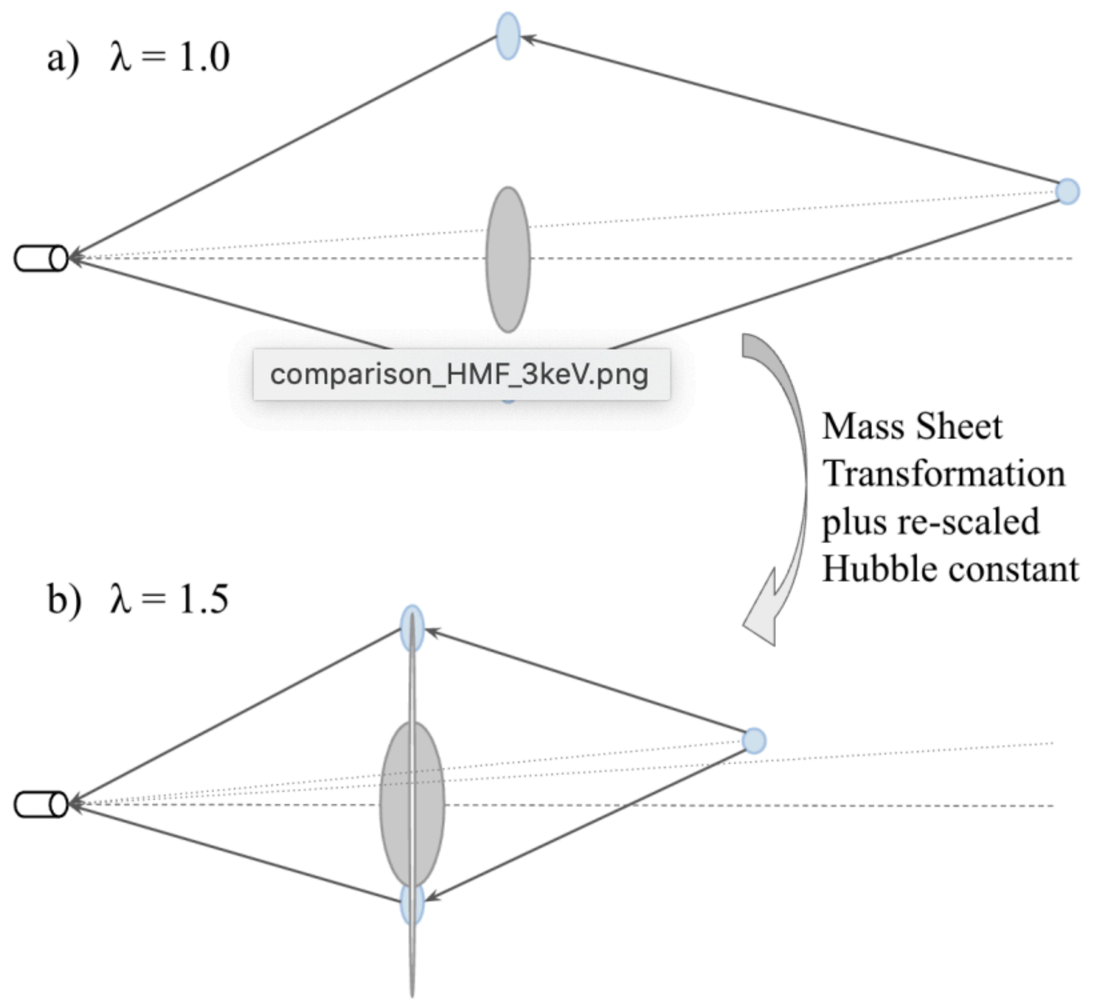

Inference goes this way:

Knowledge of z_d and z_s

↓ *(Assuming $\vec{\Omega}$)*

Compute D_d, D_s, D_{ds} as func of H_0 →

Measure Δt

↓

Lens model, knowledge of the mass profile

↓

Compute $\Delta\Phi$ →

Use $D_{\Delta t} = \frac{c\Delta t_{AB}}{\Delta\Phi_{AB}}$ to infer H_0

$$\Sigma(\Theta) \simeq \int_{\text{l.o.s.}} dz\, \rho(x,y,z)$$

Time delays - III

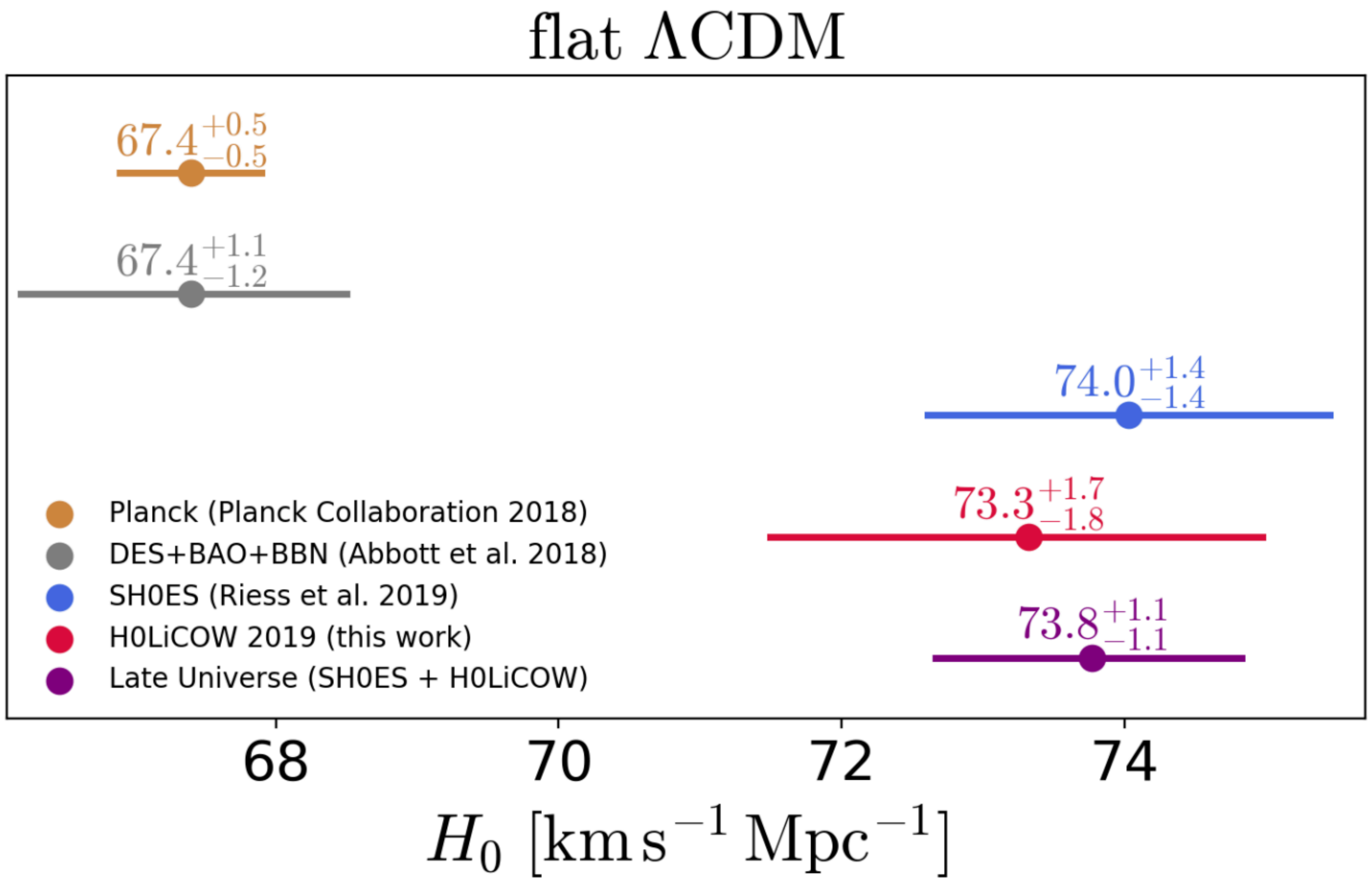

2.4% error bar on H0
5.3 sigma away from Planck value

NOTE:
Modelling of the gravitational potential

With a more flexible parametrization, H0 is only constrained if the measured time delays and imaging data are supplemented by stellar kinematics. Applying this extremely conservative choice to the TDCOSMO sample of 7 lenses increases the uncertainty on H0 from 2% to 8% --> 74 pm 6 km/s/Mpc

Deflection - I

First Derivative = 0

$$\vec{\nabla}\tau = 0$$

$$\vec{\theta} - \vec{\beta} - \vec{\nabla}\psi_{2D} = 0$$

Units=angles

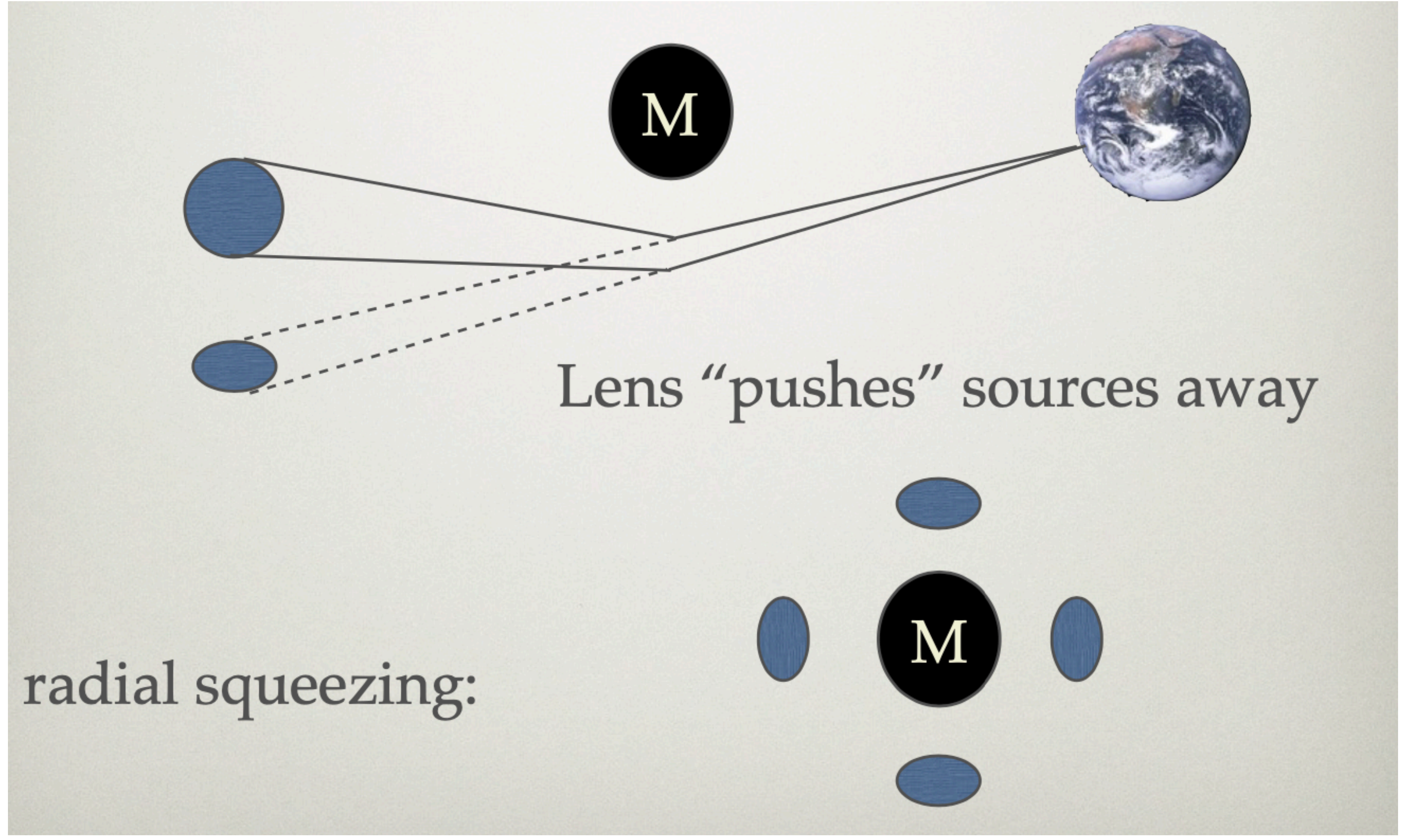

Notable example CMB lensing - from Blake Sherwin

remaps the CMB temperature: $T(\hat{\mathbf{n}})_{\rm lensed} = T(\hat{\mathbf{n}} + \mathbf{d}(\hat{\mathbf{n}}))_{\rm unlensed}$

$|\mathbf{d}(\hat{\mathbf{n}})|_{\rm filt}$

small ~3 arcminute deflections, coherent on degree scales

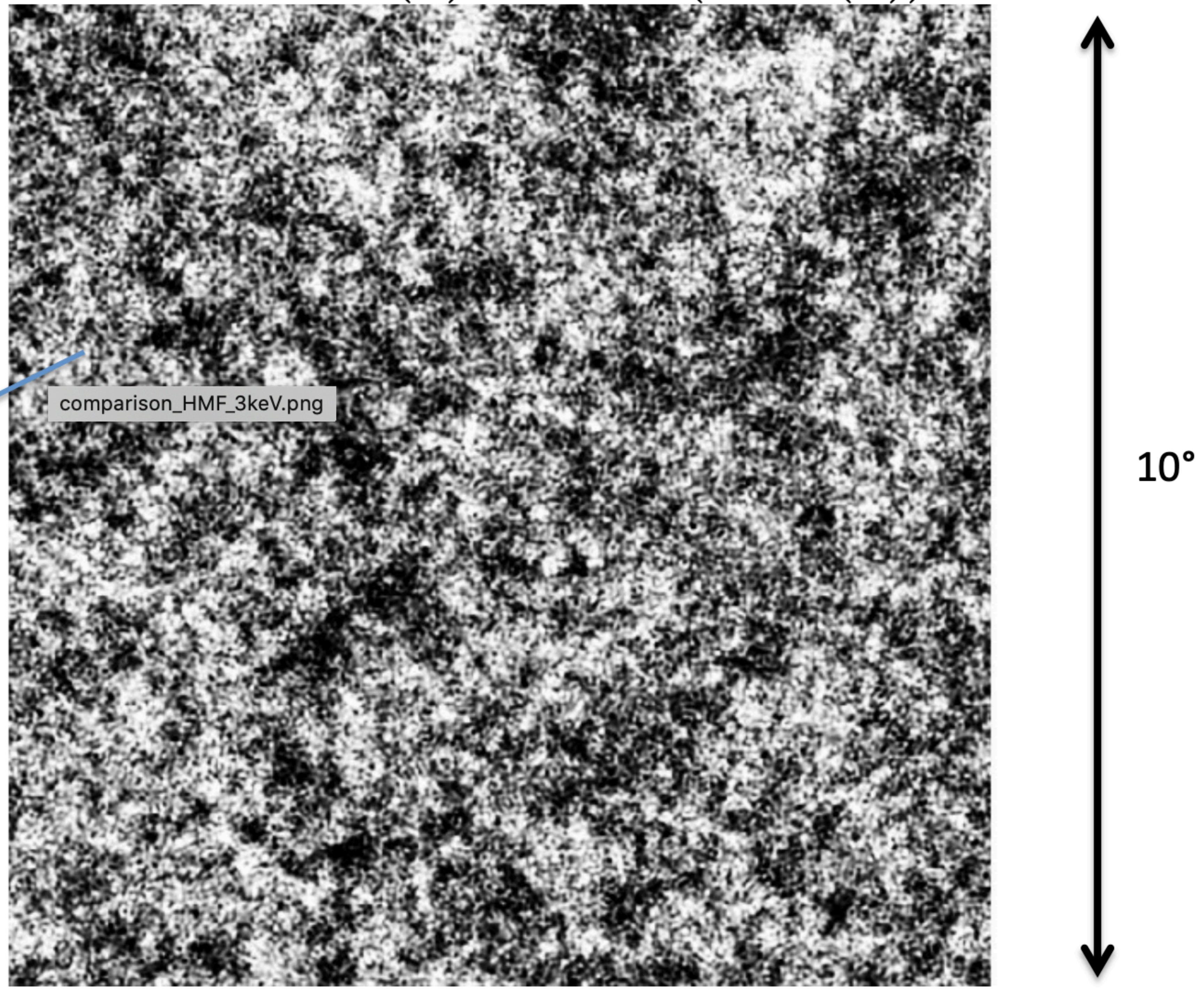

$$\nabla \cdot \underset{\text{lensing}}{d(\hat{\mathbf{n}})} = \int_0^{r_{\rm CMB}} dr \overset{\text{geometry}}{W(r)} \underset{\text{density}}{\delta(\hat{\mathbf{n}}, r)}$$

Distortion - I

The effect of lensing is to remap the images of extended sources, while conserving surface brightness

$$\frac{\partial \vec{\beta}}{\partial \vec{\theta}} = \begin{pmatrix} 1 - \frac{\partial^2 \psi}{\partial \theta_x^2} & -\frac{\partial^2 \psi}{\partial \theta_x \partial \theta_y} \\ -\frac{\partial^2 \psi}{\partial \theta_x \partial \theta_y} & 1 - \frac{\partial^2 \psi}{\partial \theta_y^2} \end{pmatrix}$$

$$\left| \frac{\partial \vec{\beta}}{\partial \vec{\theta}} \right| = 1/\mu$$

Units: angle^0

$$I(\boldsymbol{\theta}) = I^{(\mathrm{s})}[\boldsymbol{\beta}(\boldsymbol{\theta})]$$

$$I(\boldsymbol{\theta}) = I^{(\mathrm{s})}[\boldsymbol{\beta}_0 + \mathcal{A}(\boldsymbol{\theta}_0) \cdot (\boldsymbol{\theta} - \boldsymbol{\theta}_0)]$$

k is convergence
g is shear

$$\mathcal{A}(\boldsymbol{\theta}) = (1-\kappa) \begin{pmatrix} 1 - g_1 & -g_2 \\ -g_2 & 1 + g_1 \end{pmatrix}, \text{ where } g(\boldsymbol{\theta}) = \frac{\gamma(\boldsymbol{\theta})}{[1 - \kappa(\boldsymbol{\theta})]}$$

Shearing and magnification

reduced shear: $g_i = \frac{\gamma_i}{(1-\kappa)}$

magnification: $\mu = \frac{1}{\det \mathcal{A}} = \frac{1}{(1-\kappa)^2 - |\gamma|^2} = \frac{1}{(1-\kappa)^2 \, (1 - |g|^2)}$

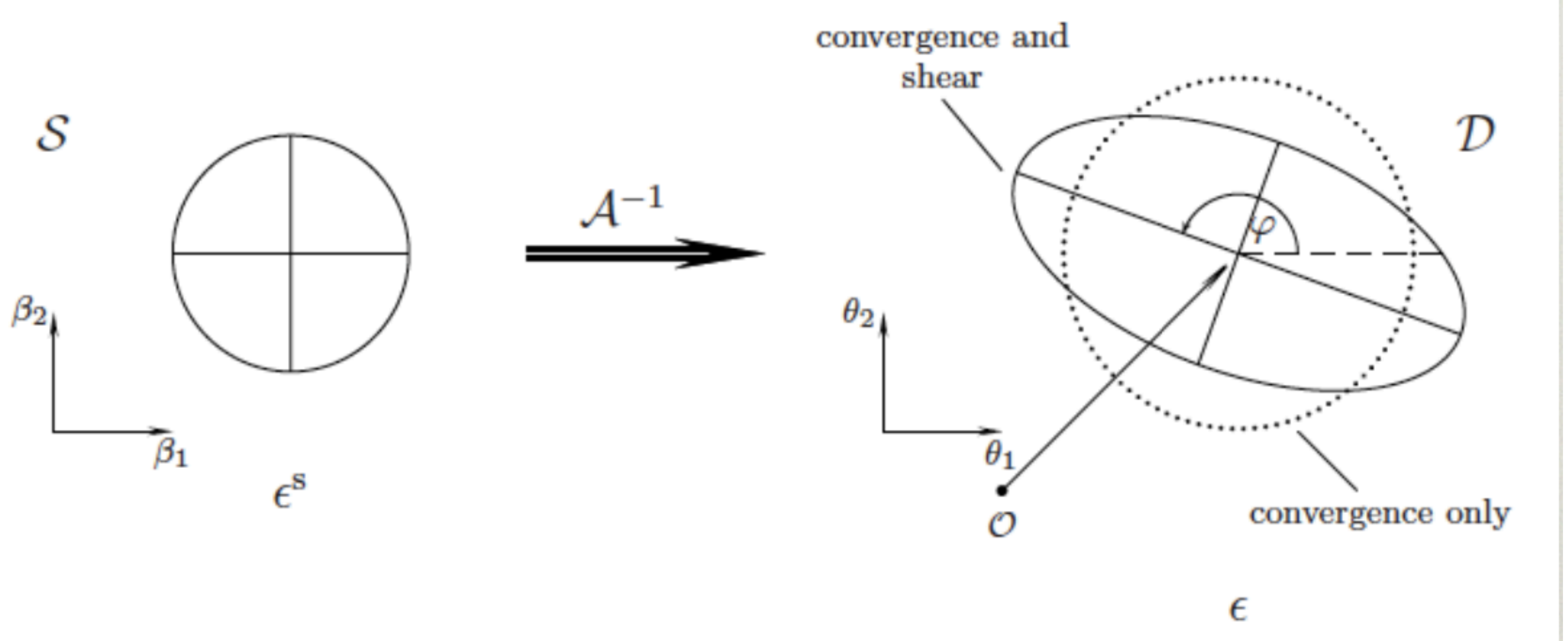

Distortion - II

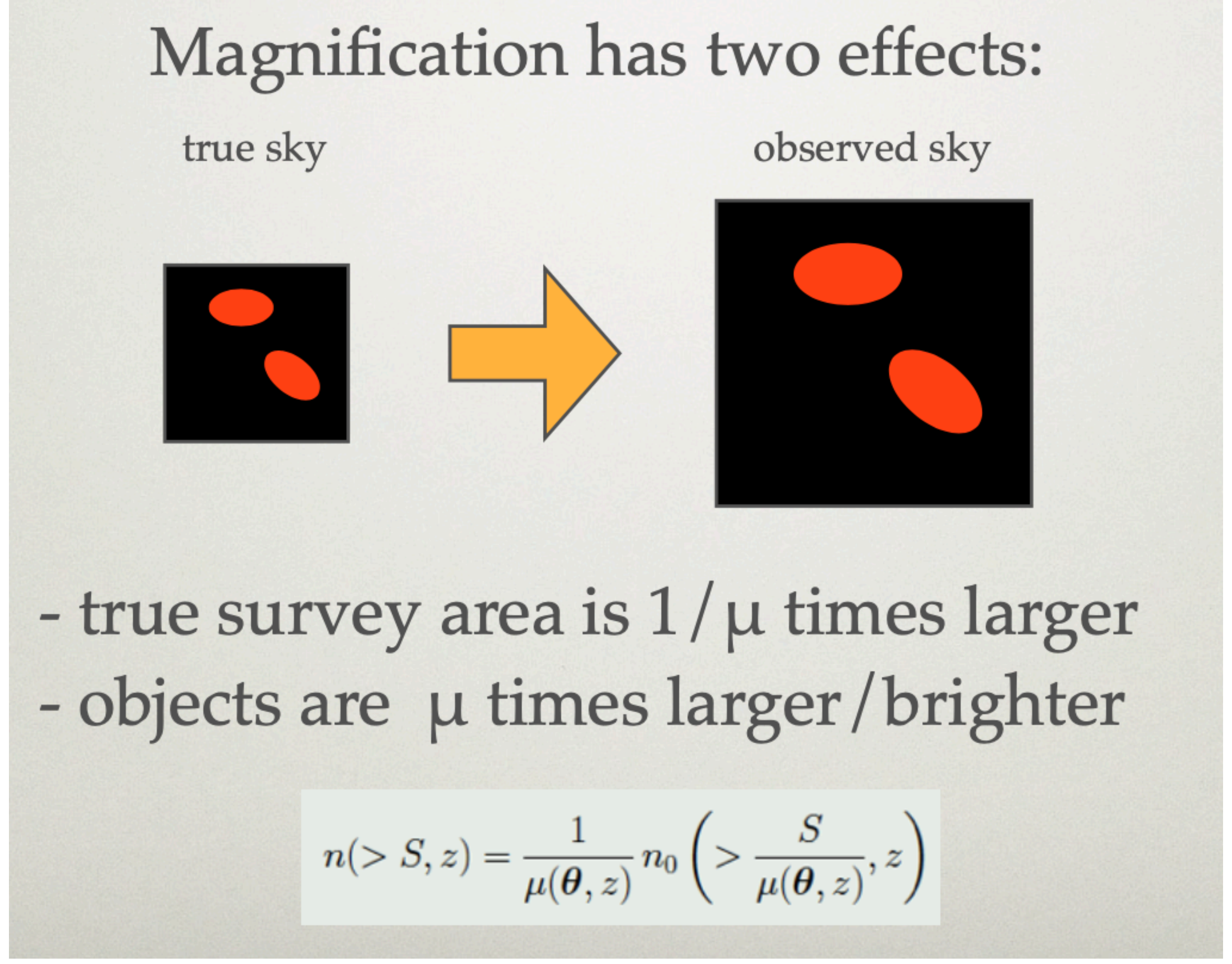

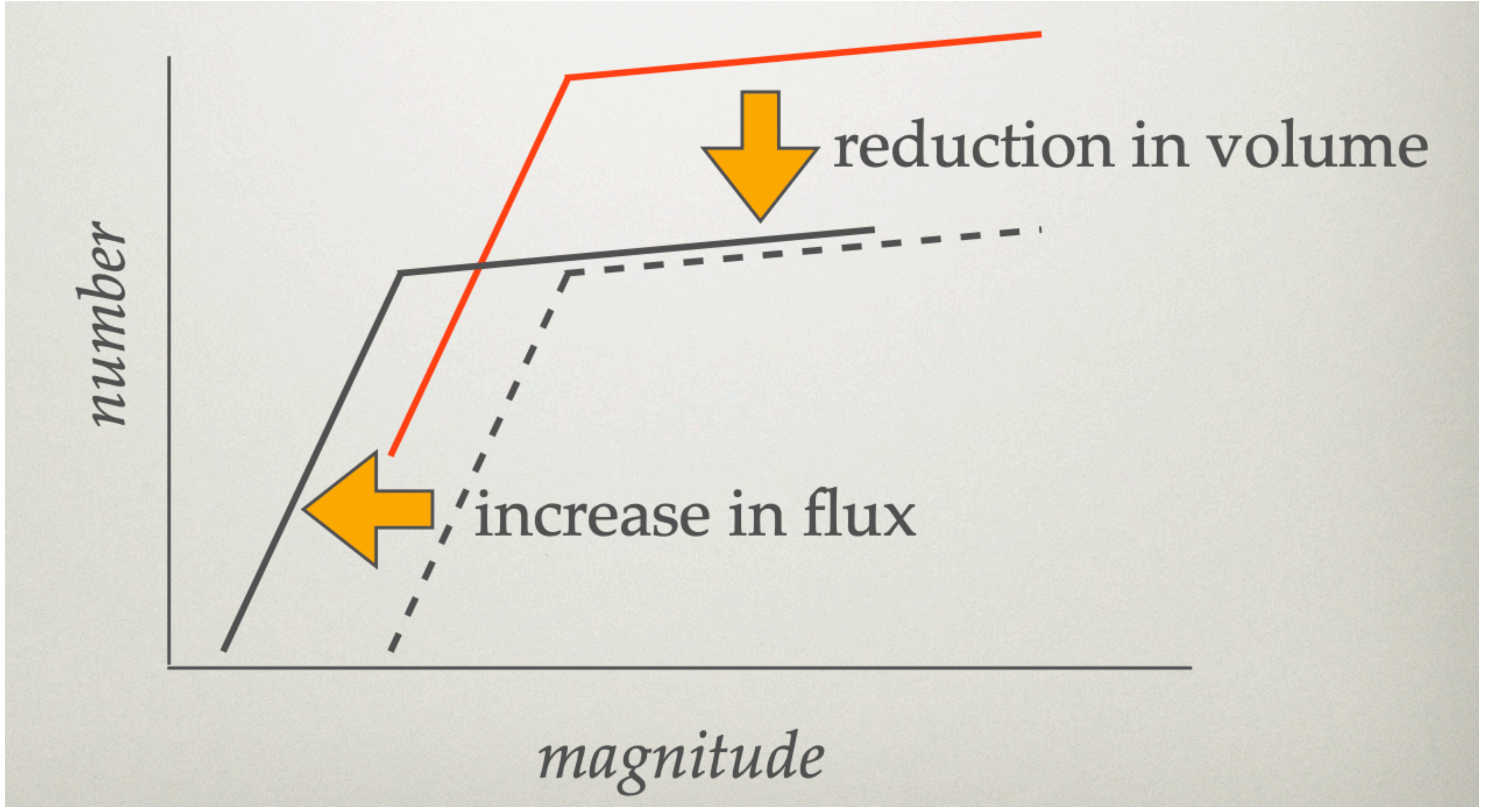

Distortion - III

GOAL: get surface density from shear (or convergence)

$$\Psi(\theta) = \frac{1}{\pi}\int d^2\vartheta \cdot \kappa(\vartheta) \ln|\theta - \vartheta|$$

$$\vec{\alpha}(\theta) = \vec{\nabla}\Psi(\theta)$$

$$\nabla^2\Psi(\theta) = 2\kappa(\theta)$$

$$\gamma_1 = \frac{1}{2}\left(\frac{\partial^2\Psi}{\partial^2 x_1} - \frac{\partial^2\Psi}{\partial^2 x_2}\right) \quad and \quad \gamma_2 = \frac{\partial^2\Psi}{\partial x_1 \partial x_2}$$

Real Space

$$\gamma(\boldsymbol{\theta}) = \frac{1}{\pi}\int_{\mathbb{R}^2} \mathrm{d}^2\theta'\, \mathcal{D}(\boldsymbol{\theta} - \boldsymbol{\theta}')\, \kappa(\boldsymbol{\theta}') \,, \quad \text{with kernel}$$

$$\mathcal{D}(\boldsymbol{\theta}) \equiv \frac{\theta_2^2 - \theta_1^2 - 2\mathrm{i}\theta_1\theta_2}{|\boldsymbol{\theta}|^4} = \frac{-1}{(\theta_1 - \mathrm{i}\theta_2)^2} \,.$$

Fourier Space

$$\hat{\gamma}(\boldsymbol{\ell}) = \pi^{-1}\hat{\mathcal{D}}(\boldsymbol{\ell})\, \hat{\kappa}(\boldsymbol{\ell}) \quad \text{for} \quad \boldsymbol{\ell} \neq \mathbf{0}$$

With inversion: $\hat{\kappa}(\boldsymbol{\ell}) = \pi^{-1}\hat{\gamma}(\boldsymbol{\ell})\, \hat{\mathcal{D}}^*(\boldsymbol{\ell}) \quad \text{for} \quad \boldsymbol{\ell} \neq \mathbf{0}$

where

$$\hat{\mathcal{D}}(\boldsymbol{\ell}) = \pi \frac{(\ell_1^2 - \ell_2^2 + 2\mathrm{i}\ell_1\ell_2)}{|\boldsymbol{\ell}|^2}$$

was used (this implies $\mathcal{D}\mathcal{D}^* = \pi^2$).

Fourier back-transformation then yields

$$\kappa(\boldsymbol{\theta}) - \kappa_0 = \frac{1}{\pi}\int_{\mathbb{R}^2} \mathrm{d}^2\theta'\, \mathcal{D}^*(\boldsymbol{\theta} - \boldsymbol{\theta}')\, \gamma(\boldsymbol{\theta}')$$

Kaiser & Squires (1993)

Distortion - IV

The shearing of images is a spin-2 field. It is useful to spend some time on the description of spin-2 fields.

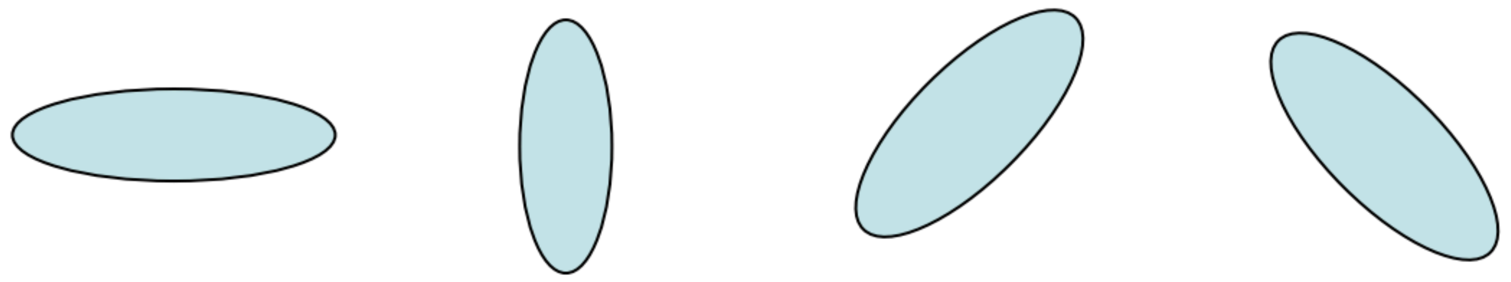

$\gamma_1>0$ $\gamma_1<0$ $\gamma_2>0$ $\gamma_2<0$

Rotating the coordinate system counterclockwise by ϕ changes

$$\gamma_1 + i\gamma_2 \rightarrow (\gamma_1 + i\gamma_2)\, e^{-2i\phi}$$

like CMB....

Keeping track of that phase as we rotate coordinates, the Fourier decomposition can be written in terms of real functions ε and β as

$$(\gamma_1 + i\gamma_2)(x) \equiv \int \frac{d^2k}{(2\pi)^2}\, [\epsilon(k) + i\beta(k)]\, e^{2i\phi_k}\, e^{i\vec{k}\cdot\vec{x}}$$

where ε is parity even and β is parity odd.

The *E*-mode is simply κ -- tangential shear around overdensities.

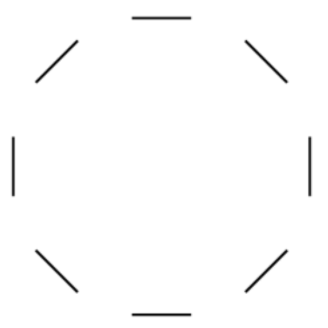

The *B*-mode is very small for gravitational lensing -- “swirling” around overdensities.

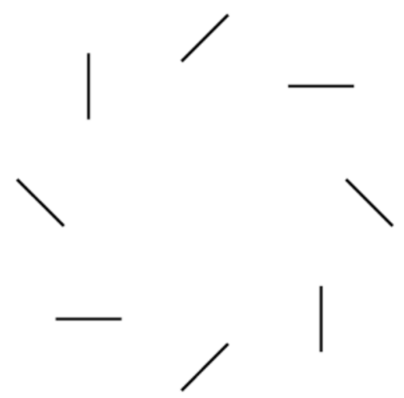

Distortion - IV

$$\langle \epsilon(\mathbf{l})\epsilon(\mathbf{l}')\rangle = (2\pi)^2\delta(\mathbf{l}-\mathbf{l}')C_l^{EE}$$
$$\langle \beta(\mathbf{l})\beta(\mathbf{l}')\rangle = (2\pi)^2\delta(\mathbf{l}-\mathbf{l}')C_l^{BB}$$
$$\langle \epsilon(\mathbf{l})\beta(\mathbf{l}')\rangle = (2\pi)^2\delta(\mathbf{l}-\mathbf{l}')C_l^{EB}$$

$$\langle \gamma_t \rangle(\theta) = \bar{\kappa}(\theta) - \langle \kappa \rangle(\theta)$$

Using Gauss theorem

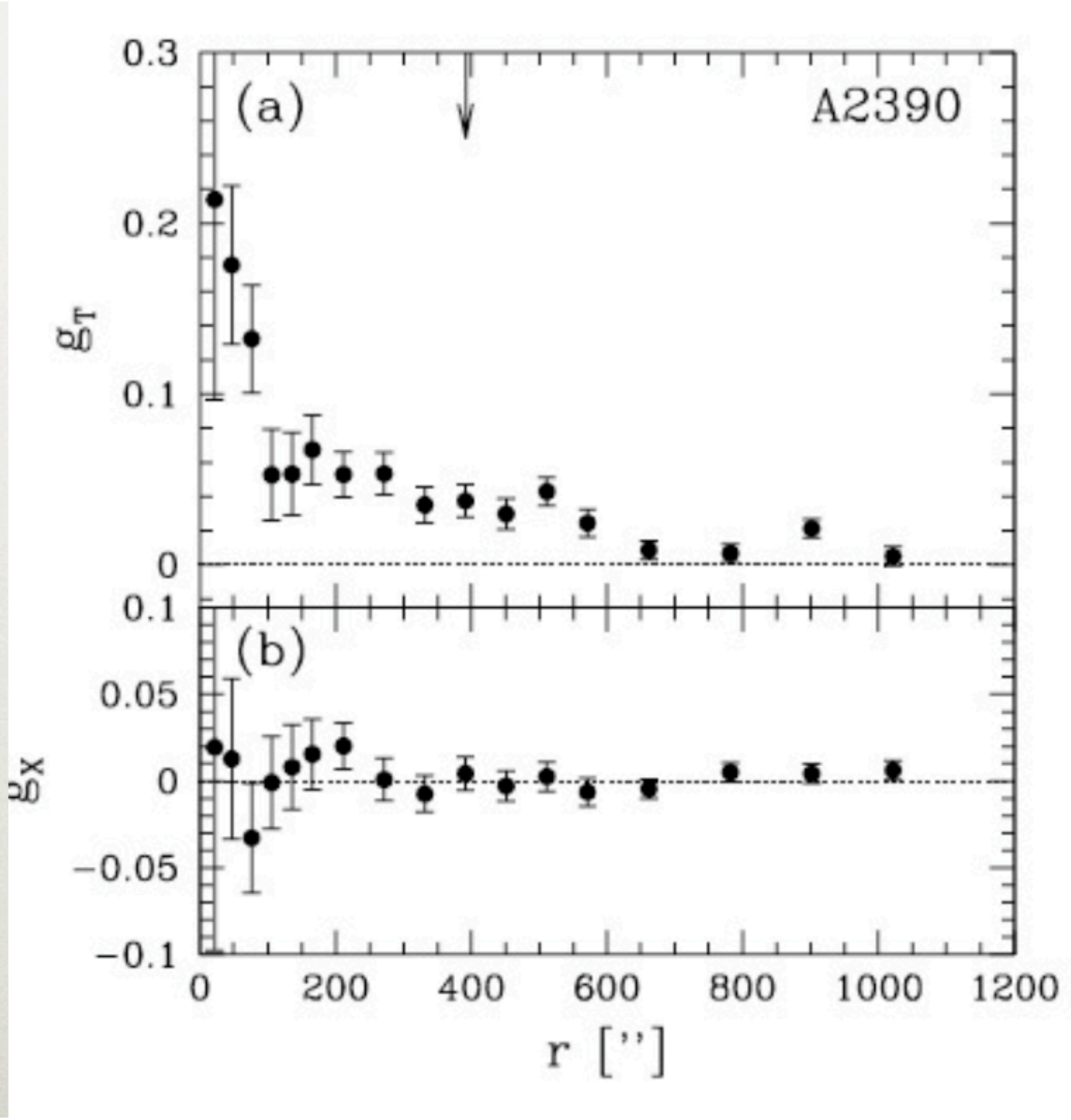

The tangential shear provides a direct measure of the mass contrast. It is a local measurement. This can be used to estimate projected masses within a radius with minimal assumptions about the radial matter distribution.

COSMOLOGY WITH WEAK LENSING

In context

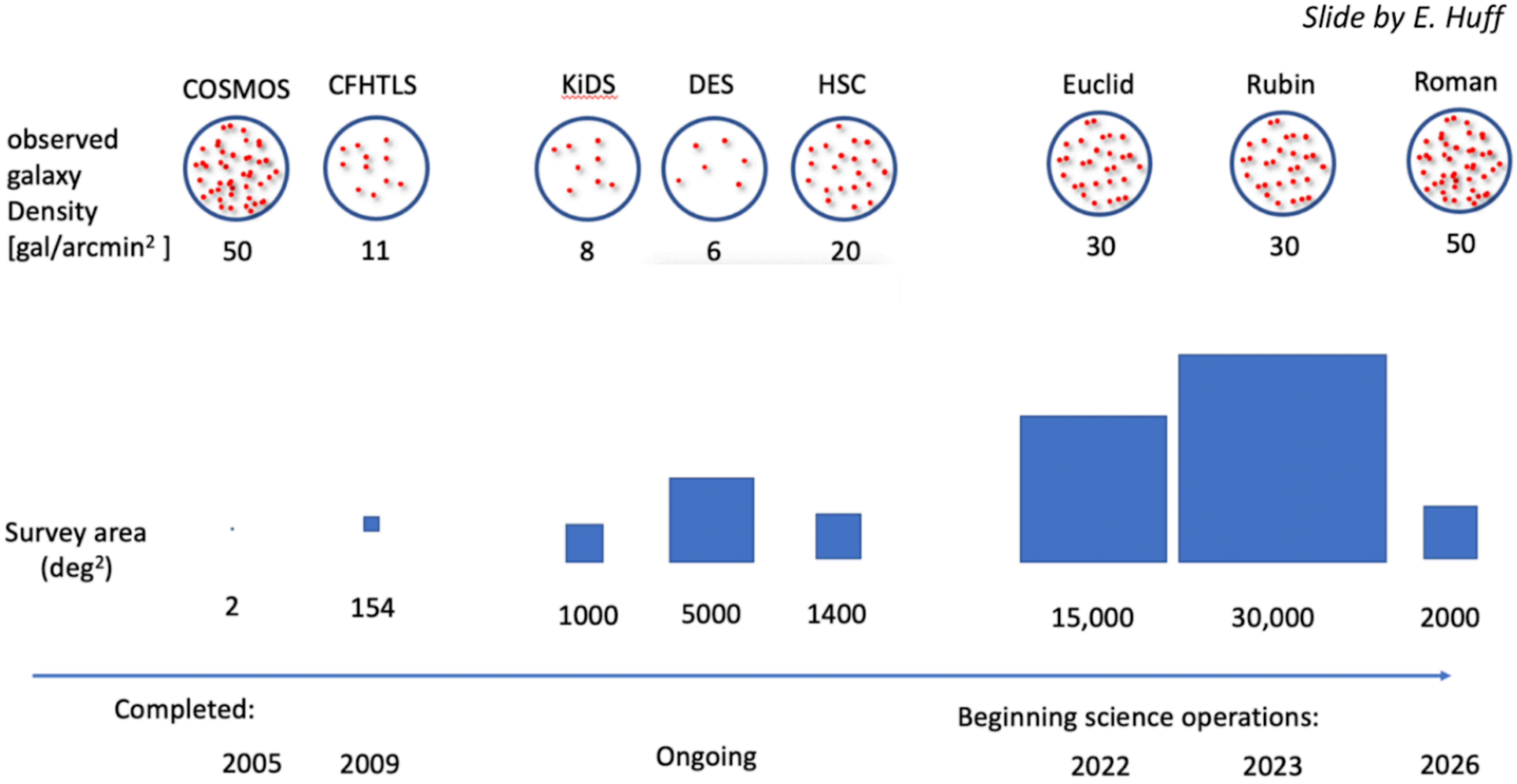

Slide by E. Huff
COSMOS
CFHTLS
KiDS
DES
HSC
Euclid
Rubin
Roman
observed galaxy Density [gal/arcmin²]
50
11
8
6
20
30
30
50
Survey area (deg²)
2
154
1000
5000
1400
15,000
30,000
2000
Completed:
2005
2009
Ongoing
Beginning science operations:
2022
2023
2026

The Dark Energy Survey (DES)

- 570 Megapixel camera for the Blanco 4m telescope in Chile.
- Observed in 5 imaging bands (grizY) : photometric redshifts
- Full survey 758 nights (2013-19)
- This talk DES Y3 (2013-16).
- **Wide field:** 5000 sq. deg. with limiting depth i <~ 24
- **Deep field:** 30 sq. deg. with near-IR YJHK bands, 10x wide field depth

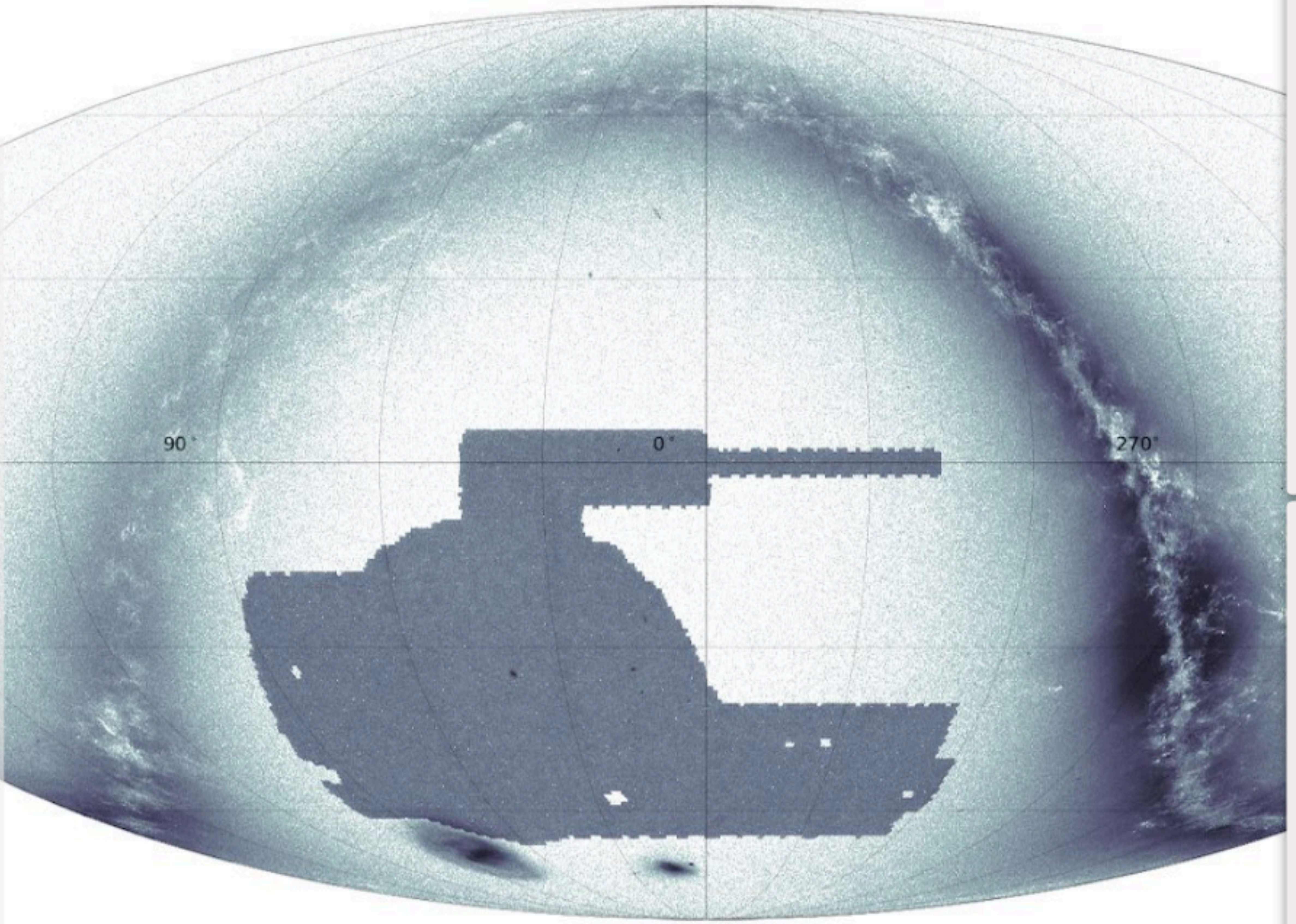

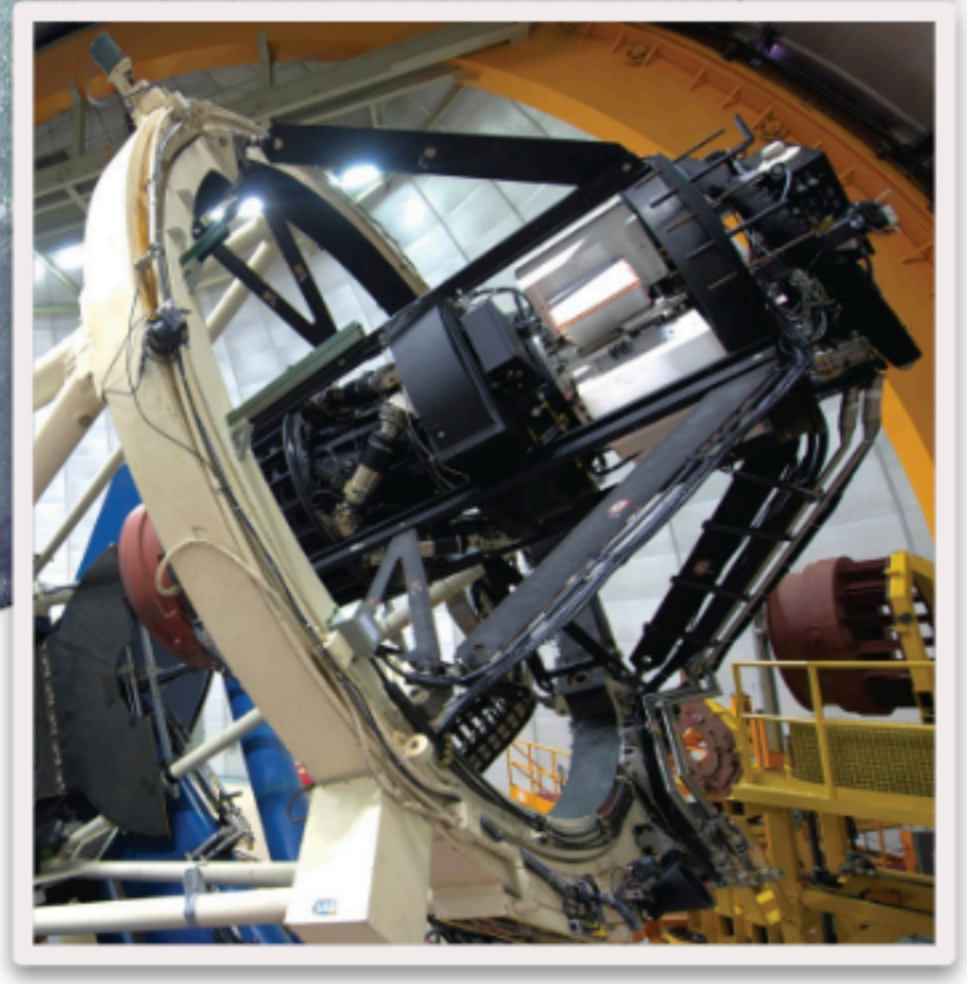

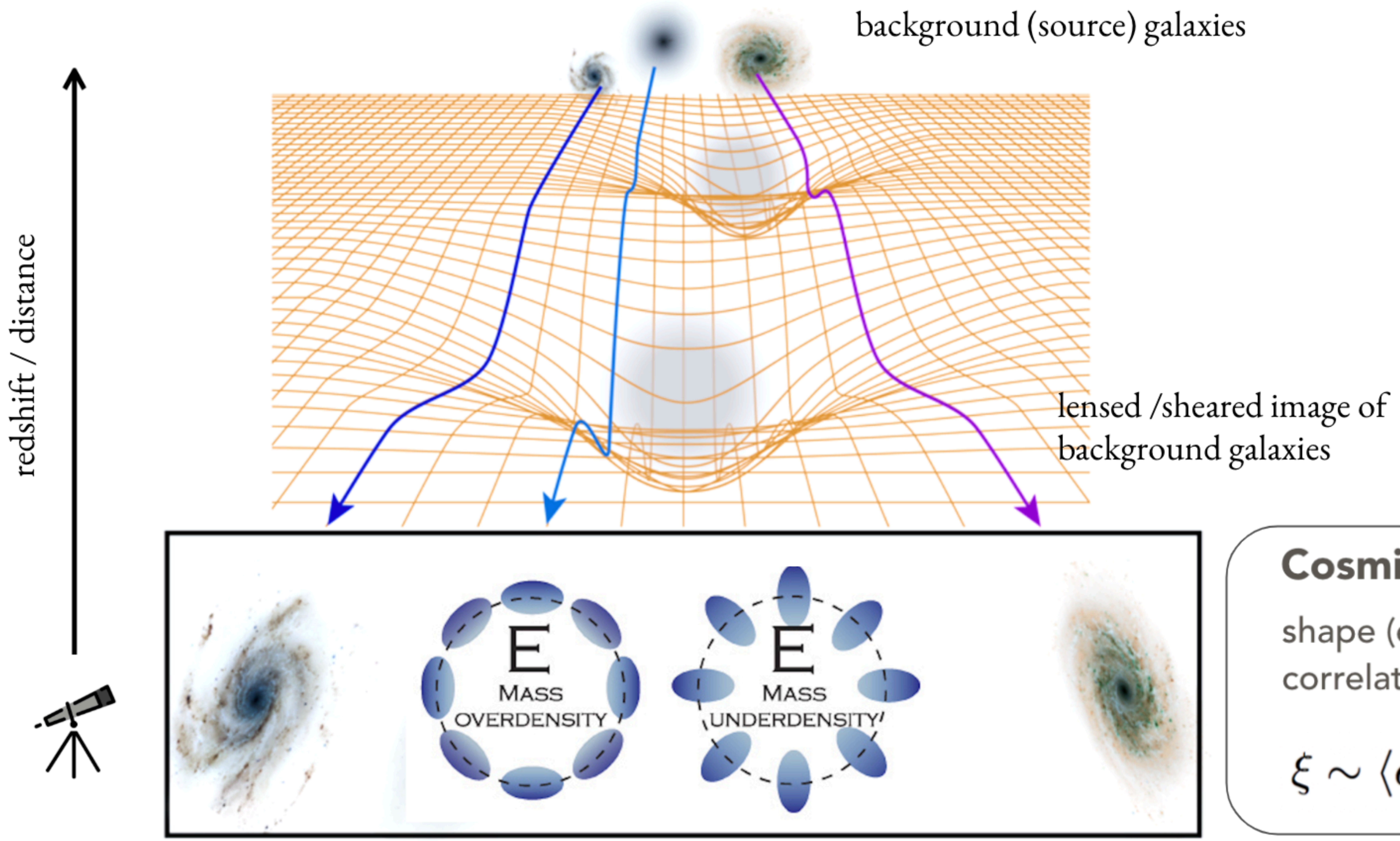

Cosmic Shear

shape (ellipticity) - shape correlation

$$\xi \sim \langle e(\theta')e(\theta' + \theta)\rangle$$

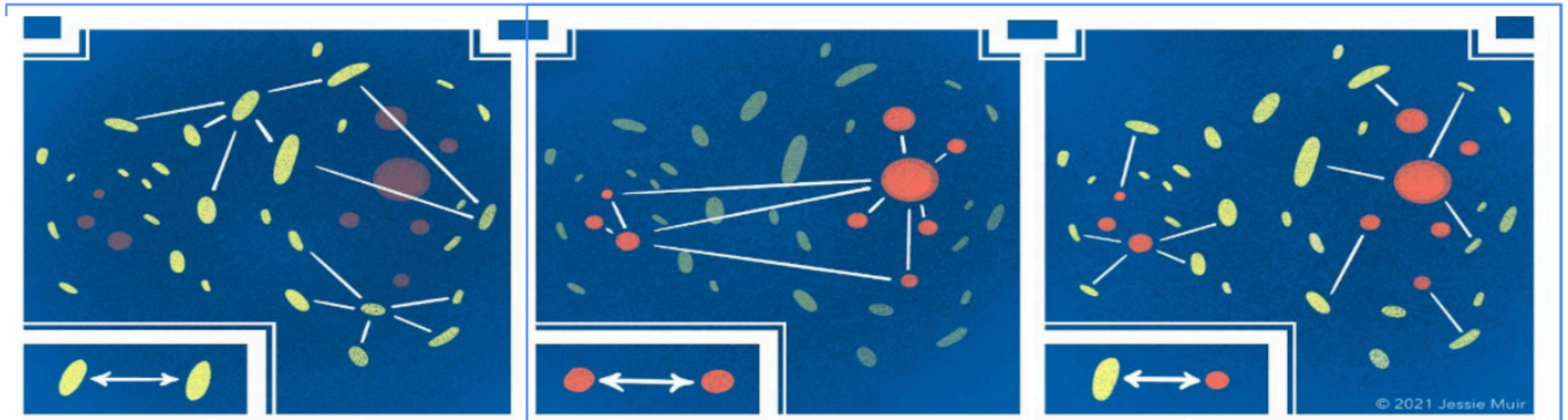

cosmic shear

correlation in the shapes of (source) galaxies

$$\xi_\pm = \langle e_\mathrm{t}(\theta')e_\mathrm{t}(\theta'+\theta)\rangle - \langle e_\mathrm{x}(\theta')e_\mathrm{x}(\theta'+\theta)\rangle$$

$$\propto \sigma_8^2$$

galaxy clustering

correlation in the positions of (lens) galaxies

$$w(\theta) = \langle \delta(\theta')\delta(\theta'+\theta)\rangle$$

$$\propto b^2\sigma_8^2$$

galaxy-galaxy lensing

correlation between positions of the lenses and shapes of the sources

$$\gamma_t(\theta) = \langle \delta(\theta')e_\mathrm{t}(\theta'+\theta)\rangle$$

$$\propto b\sigma_8^2$$

1x2pt

2x2pt

3x2pt

Cosmology!

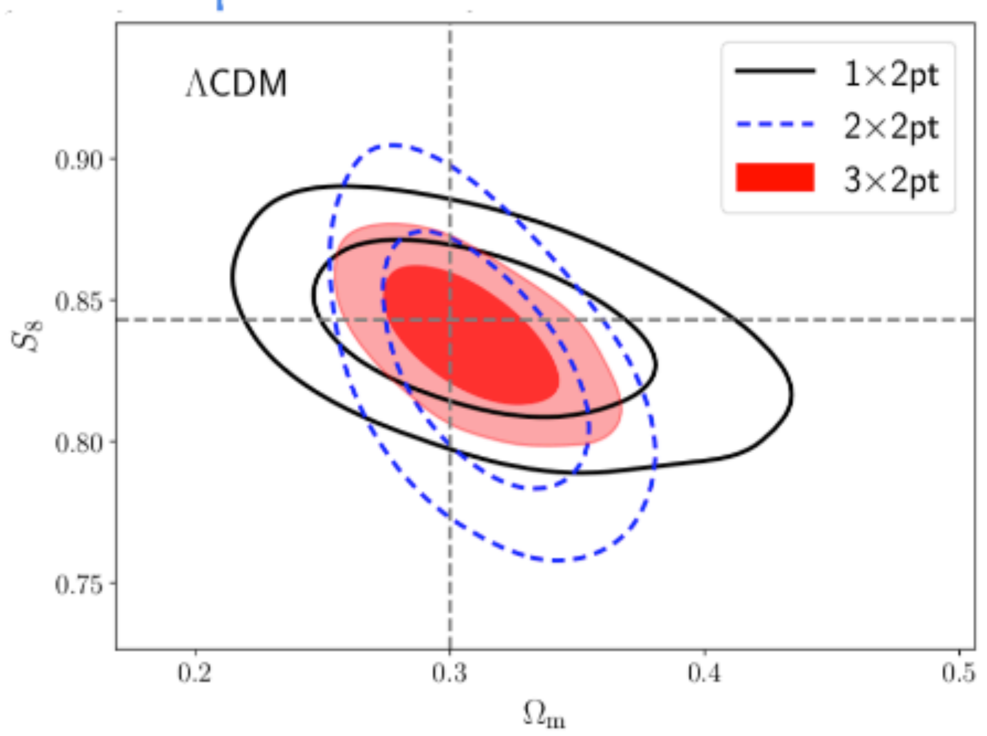

3x2pt Data-vector

DES uses correlation functions in angular or configuration space.

$$w^i(\theta) = \sum_\ell \mathcal{G}_0\left(\ell, \theta_{\min}, \theta_{\max}\right) C^{ii}_{\delta_{\text{obs}}\delta_{\text{obs}}}(\ell)$$

$$\gamma_{\text{t}}^{ij}(\theta) = \sum_\ell \mathcal{G}_2\left(\ell, \theta_{\min}, \theta_{\max}\right) C^{ij}_{\delta_{\text{obs}}\text{E}}(\ell)$$

$$\xi_\pm^{ij}(\theta) = \sum_\ell \mathcal{G}_{4,\pm}\left(\ell, \theta_{\min}, \theta_{\max}\right) \left[C^{ij}_{\text{EE}}(\ell) \pm C^{ij}_{\text{BB}}(\ell)\right]$$

From 4 lens and 4 source tomographic bins we get $\hat{\mathbf{D}} \equiv \{\hat{w}^i(\theta), \hat{\gamma}_{\text{t}}^{ij}(\theta), \hat{\xi}_\pm^{ij}(\theta)\}$

- 4 auto correlation functions for clustering
- 10 bin paris for galaxy-galaxy lensing
- 10 bin pairs fro cosmic shear+ and 10 bin pairs for cosmic shear-

462 data-points after scale-cuts with a total S/N = 87 (twice DESY1)

How beautiful!!!

....but in practice....

"I know I'm out of touch with reality.
That's my best stress-management technique!"

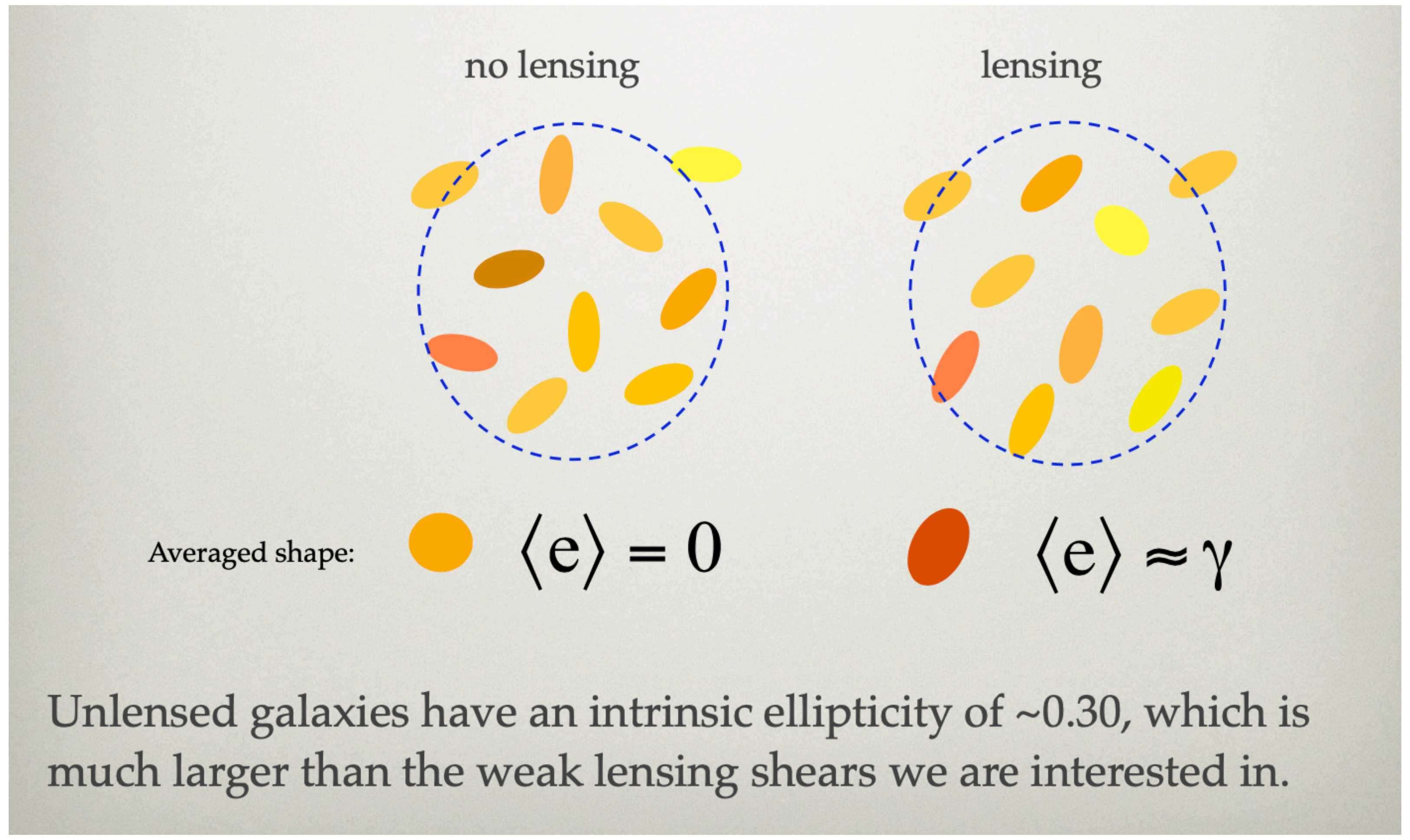

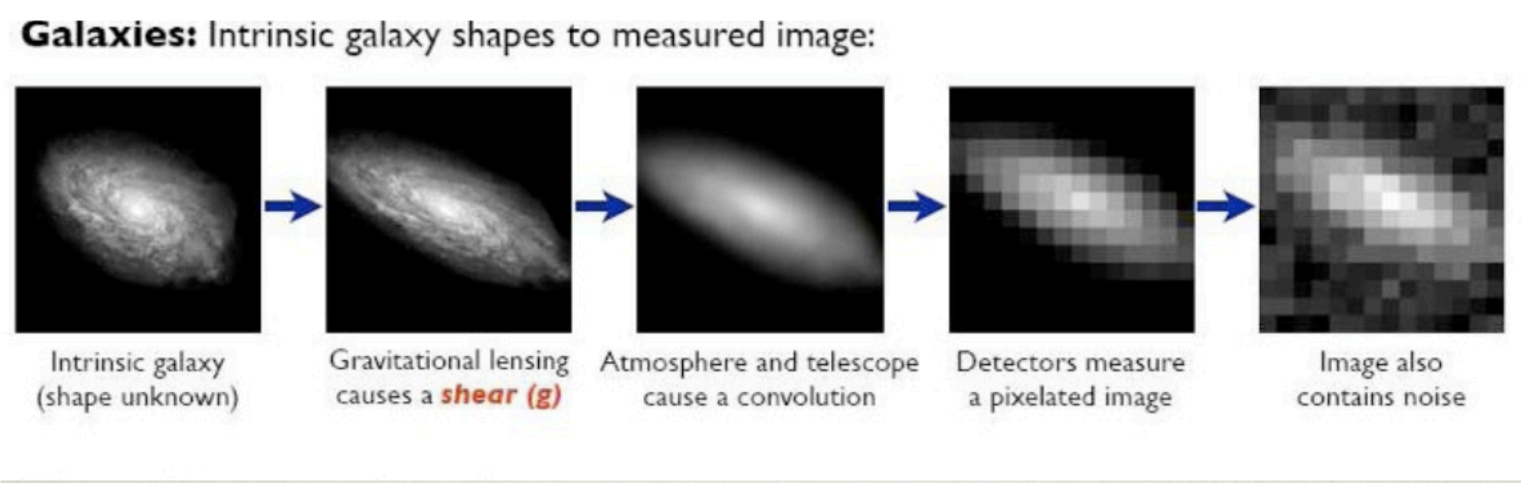

- Linear galaxy bias only valid on large scales
- Galaxies intrinsically aligned (not randomly oriented)
- Estimating galaxy distances through photometric redshifts in few bands
- Measuring and deconvolving the Point Spread Functions (PSF)
- Shear estimations biases → calibration with image simulations
- Galaxy images blend
- Blending couples with photometric redshifts
- Galaxy images are taken with a wide range of observing conditions
- Observing conditions imprint large-scale density fluctuations

3x2pt Data + Model fit

cosmic shear **Amon,+(2021),Secco,Samuroff,+(2021)**

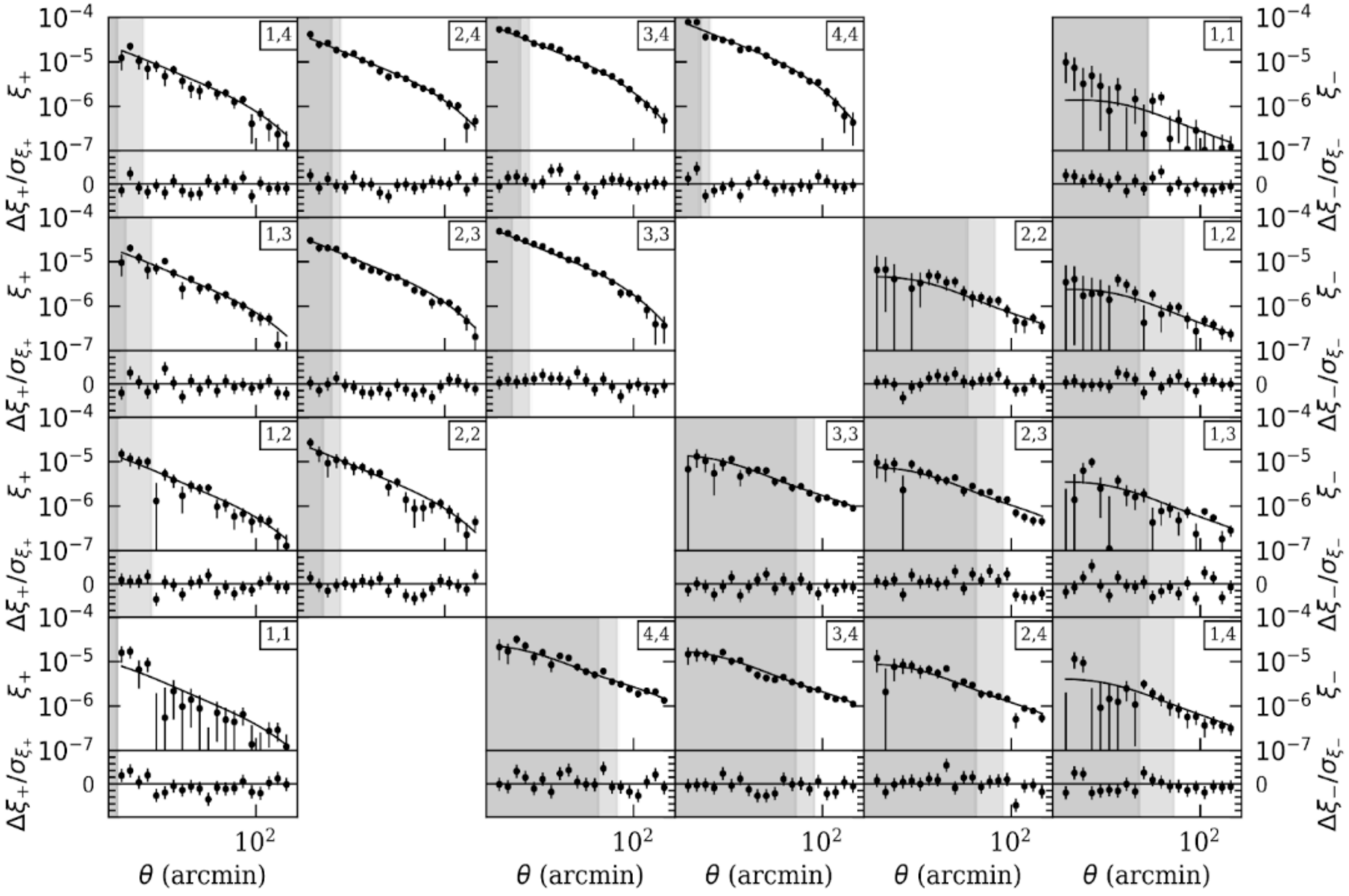

galaxy-galaxy lensing **Prat,+(2021)**

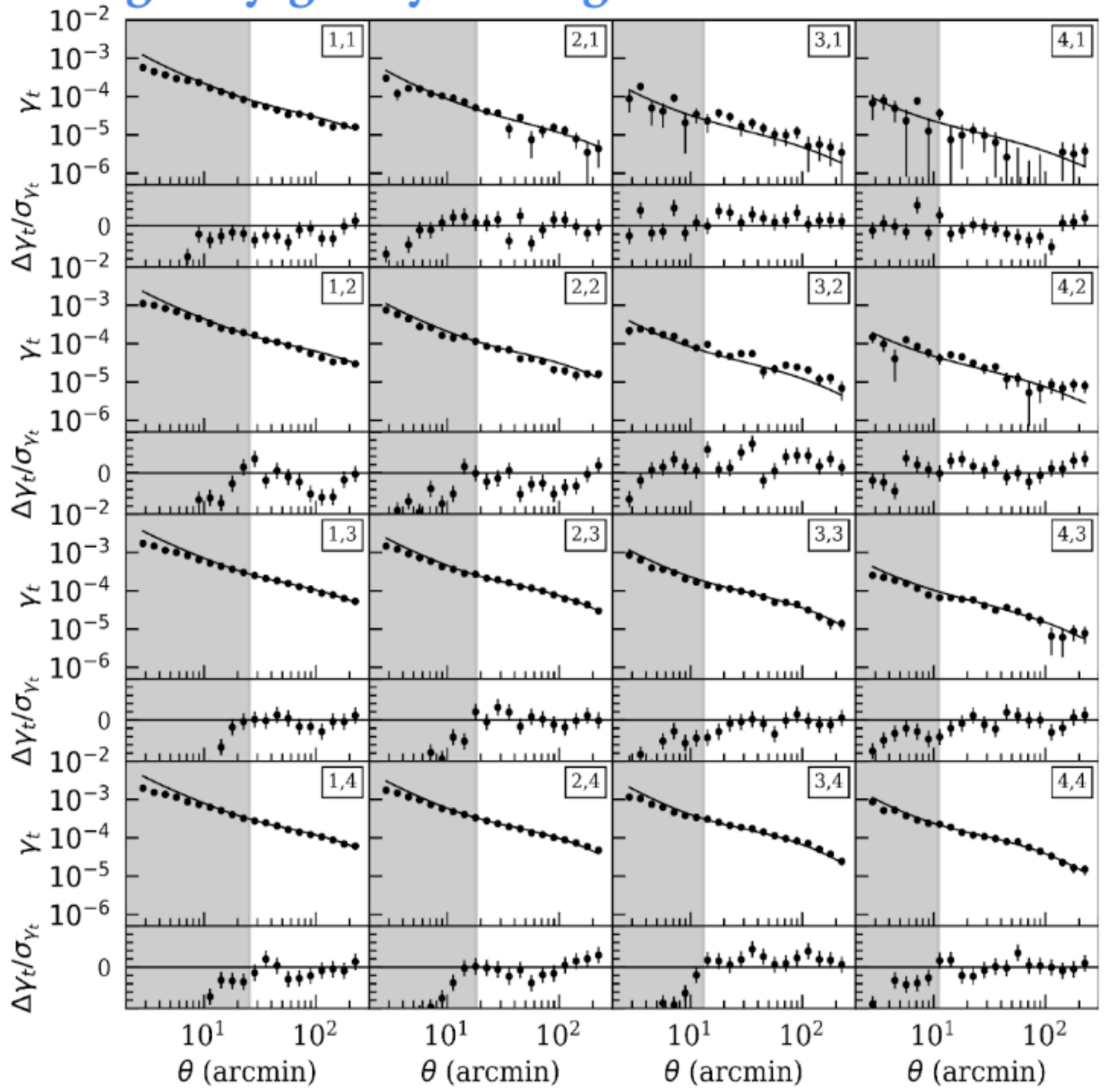

galaxy clustering **Rodriguez-Monroy,+(2021)**

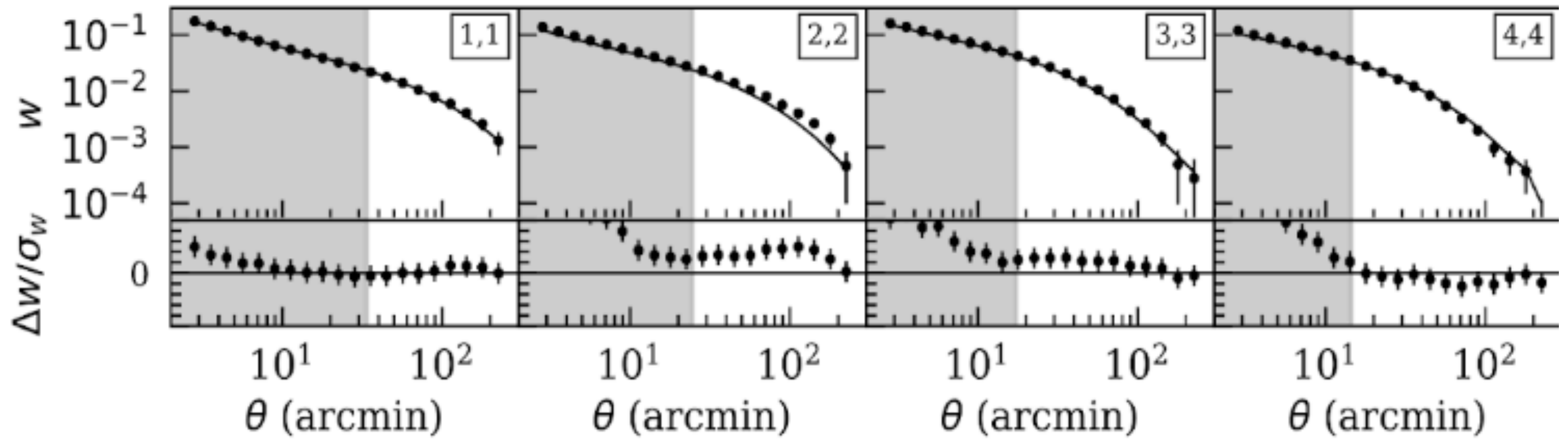

Internal consistency

Two correlated cosmological probes:

1. **Cosmic shear** (blue)
2. **Galaxy clustering** and **tangential shear** (orange)

We find consistency between them.

Cosmic shear most sensitive to clustering amplitude.

Galaxy clustering and tangential shear more sensitive to total matter density.

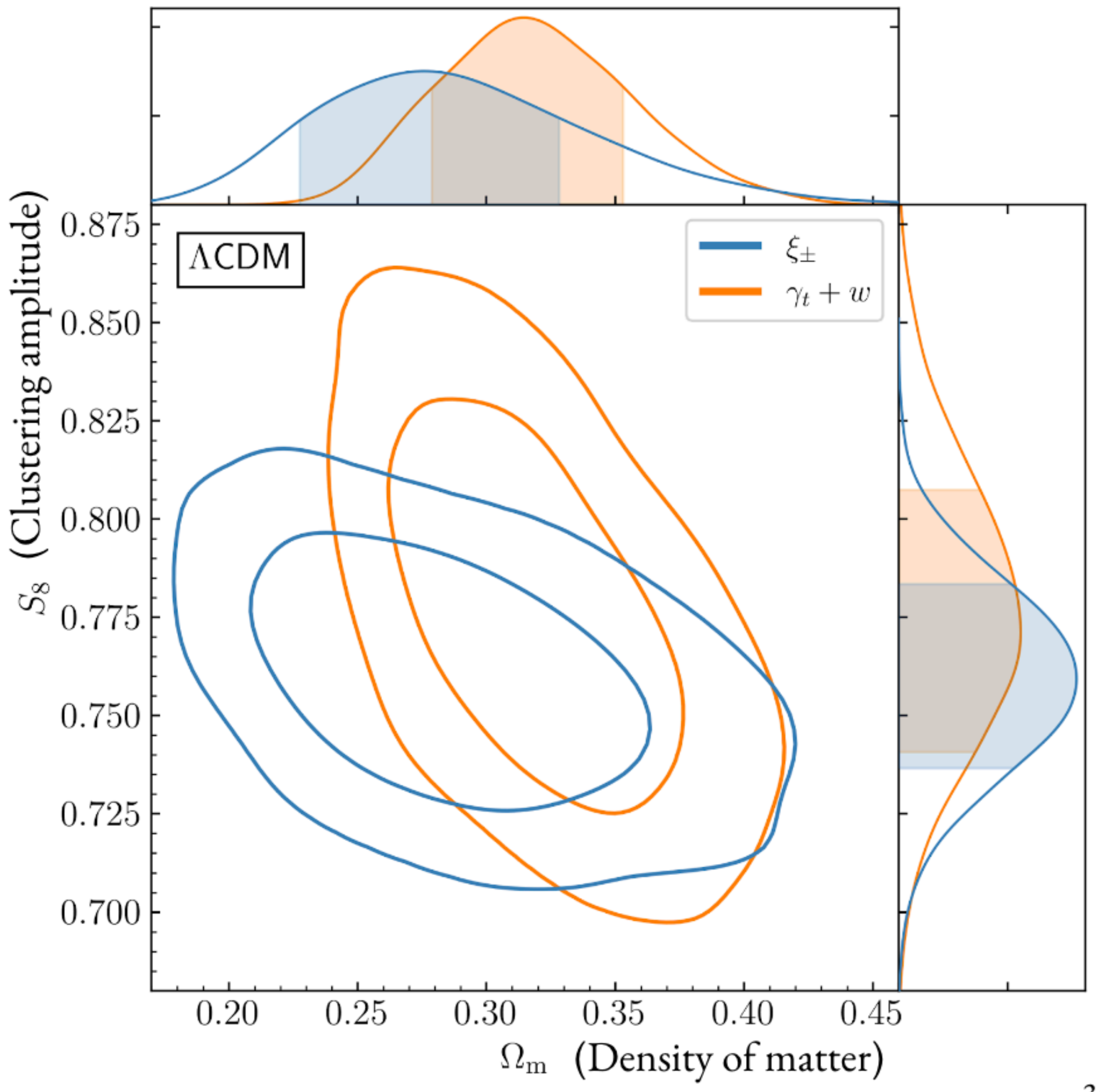

DES only 3x2pt results

We combine these into the **3x2pt** probe of large-scale structure.

A factor of 2.1 improvement in signal-to-noise from DES Year 1 (and in the $\sigma_8 - \Omega_m$ plane).

In ΛCDM:

$$S_8 = 0.776^{+0.017}_{-0.017} \quad (0.776)$$

$$\Omega_m = 0.339^{+0.032}_{-0.031} \quad (0.372)$$

$$\sigma_8 = 0.733^{+0.039}_{-0.049} \quad (0.696)$$

In wCDM:

$$\Omega_m = 0.352^{+0.035}_{-0.041} \quad (0.339)$$

$$w = -0.98^{+0.32}_{-0.20} \quad (-1.03)$$

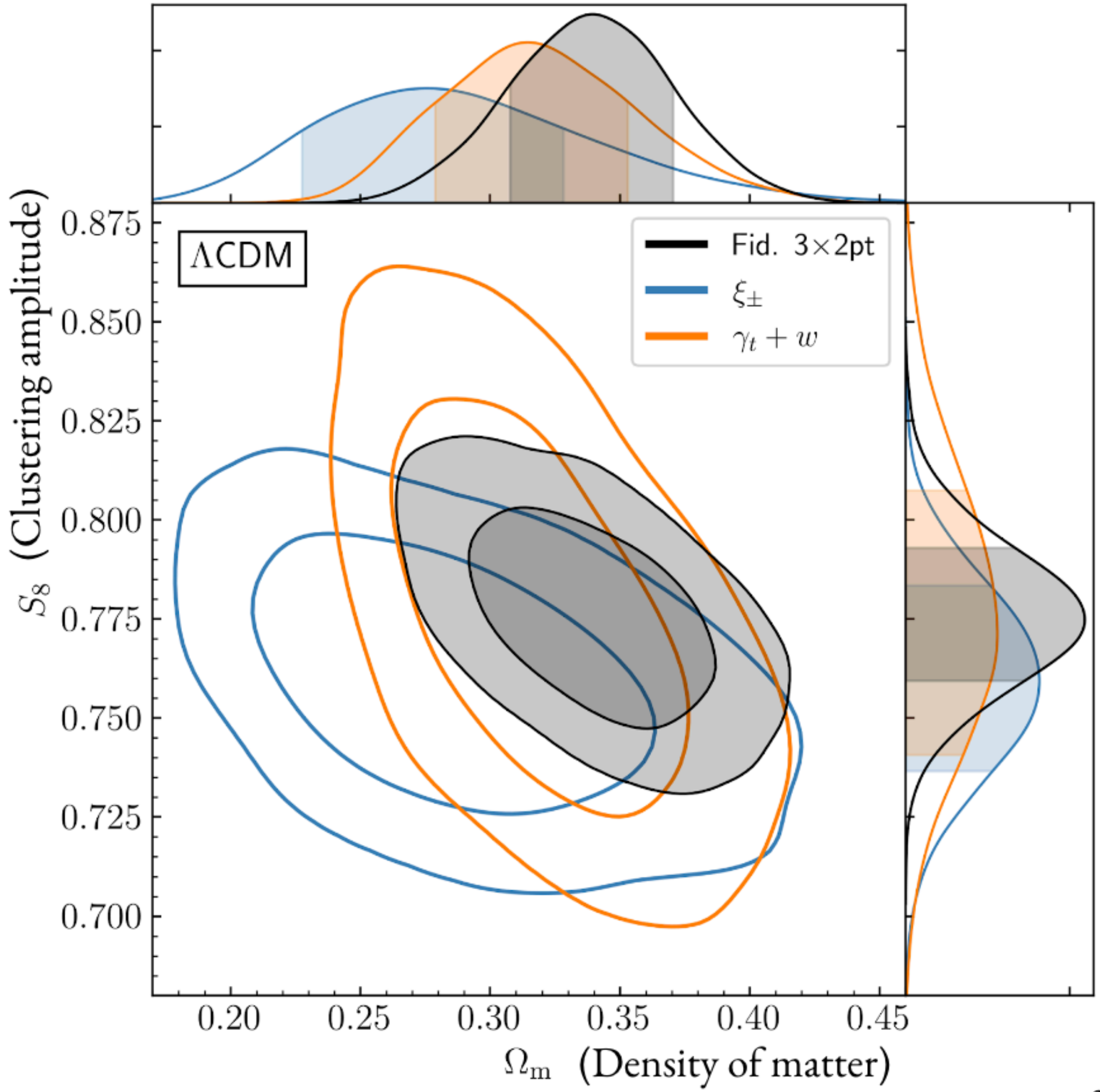

Low-z vs High-z in ΛCDM

We test the robustness of ΛCDM by comparing measurements of the clustering amplitude at low-redshift to the prediction from the cosmic microwave background (CMB) at high-redshift.

We find no significant evidence of inconsistency between **DES Y3 3x2pt** and *Planck* CMB at 1.5σ (p-value=0.13). Cosmic shear only at 2.1σ

Suspiciousness of 0.7σ (p-value = 0.48).

Roughly similar as in DESY1 but with an increase in precision in both probes.

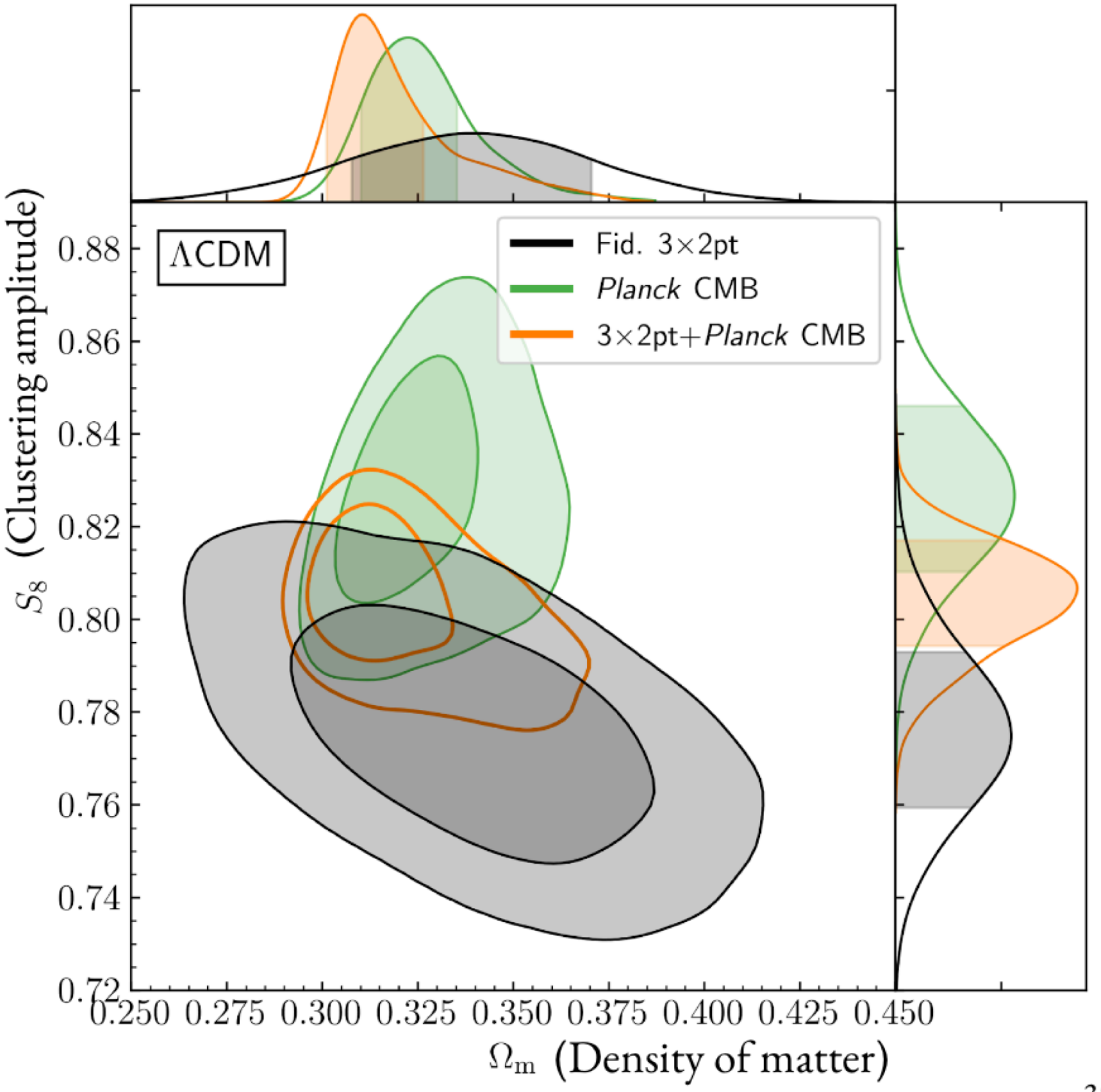

The *Hubble* parameter tension

Local measurements of h, e.g. from Cepheids variable stars (SHOES collab.), with MIRA variable stars, masers, strong lensing time delays, etc tend to find higher h values than derived by CMB observations at high-z assuming LCDM

BAO+BBN+DES 3x2 similar constraining power as *Planck* CMB, all combined leads to

$$h = 0.680^{+0.004}_{-0.003}$$

Roughly 4σ smaller than SHOES

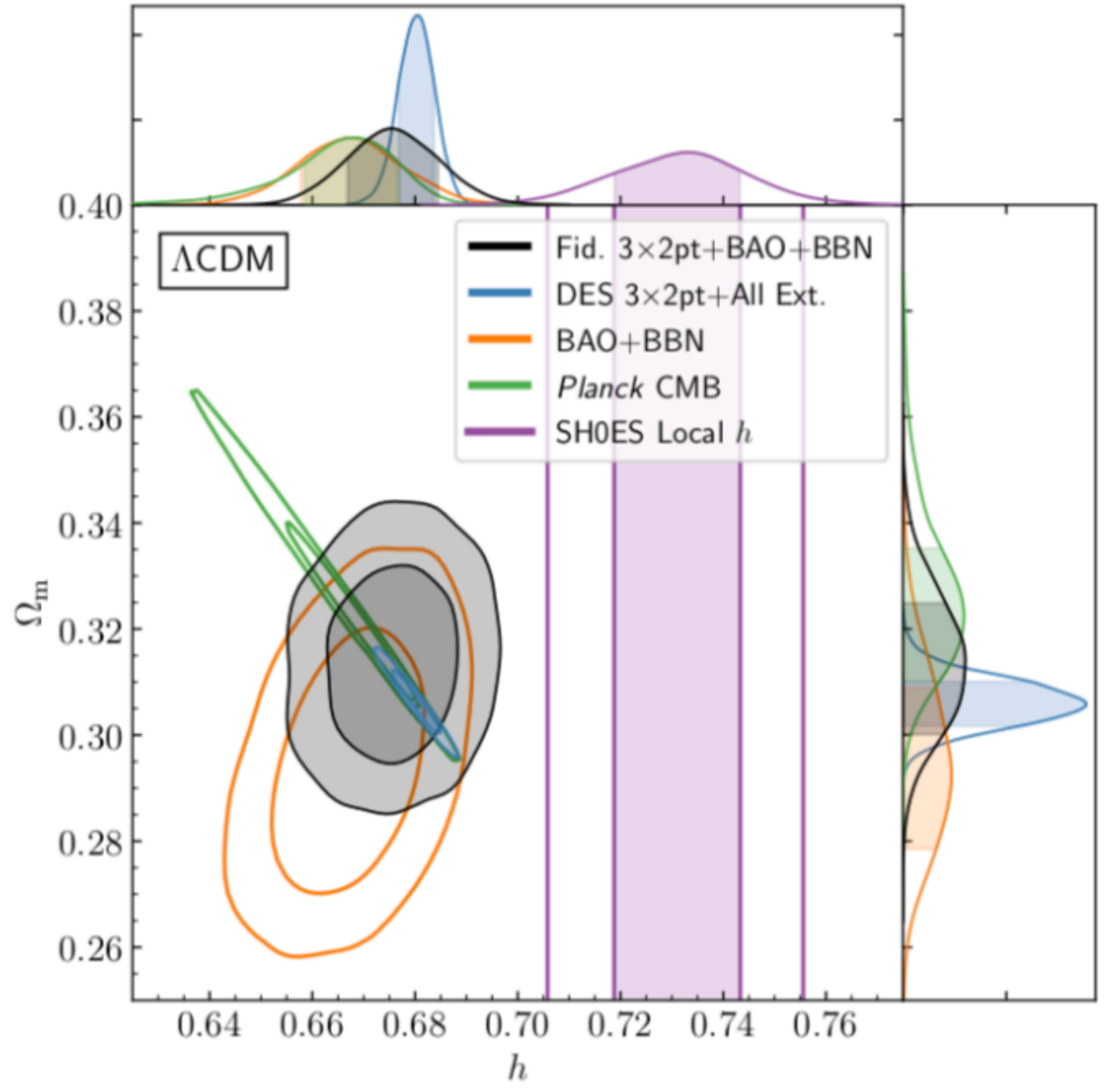

Joint constraints

Combining all these data sets we find:

In ΛCDM:

$$S_8 = 0.812^{+0.008}_{-0.008} \quad (0.815)$$

$$\Omega_\mathrm{m} = 0.306^{+0.004}_{-0.005} \quad (0.306)$$

$$\sigma_8 = 0.804^{+0.008}_{-0.008} \quad (0.807)$$

$$h = 0.680^{+0.004}_{-0.003} \quad (0.681)$$

$$\sum m_\nu < 0.13 \text{ eV (95\% CL)}$$

In wCDM:

$$\sigma_8 = 0.810^{+0.010}_{-0.009} \quad (0.804),$$

$$\Omega_\mathrm{m} = 0.302^{+0.006}_{-0.006} \quad (0.298),$$

$$w = -1.03^{+0.03}_{-0.03} \quad (-1.00)$$

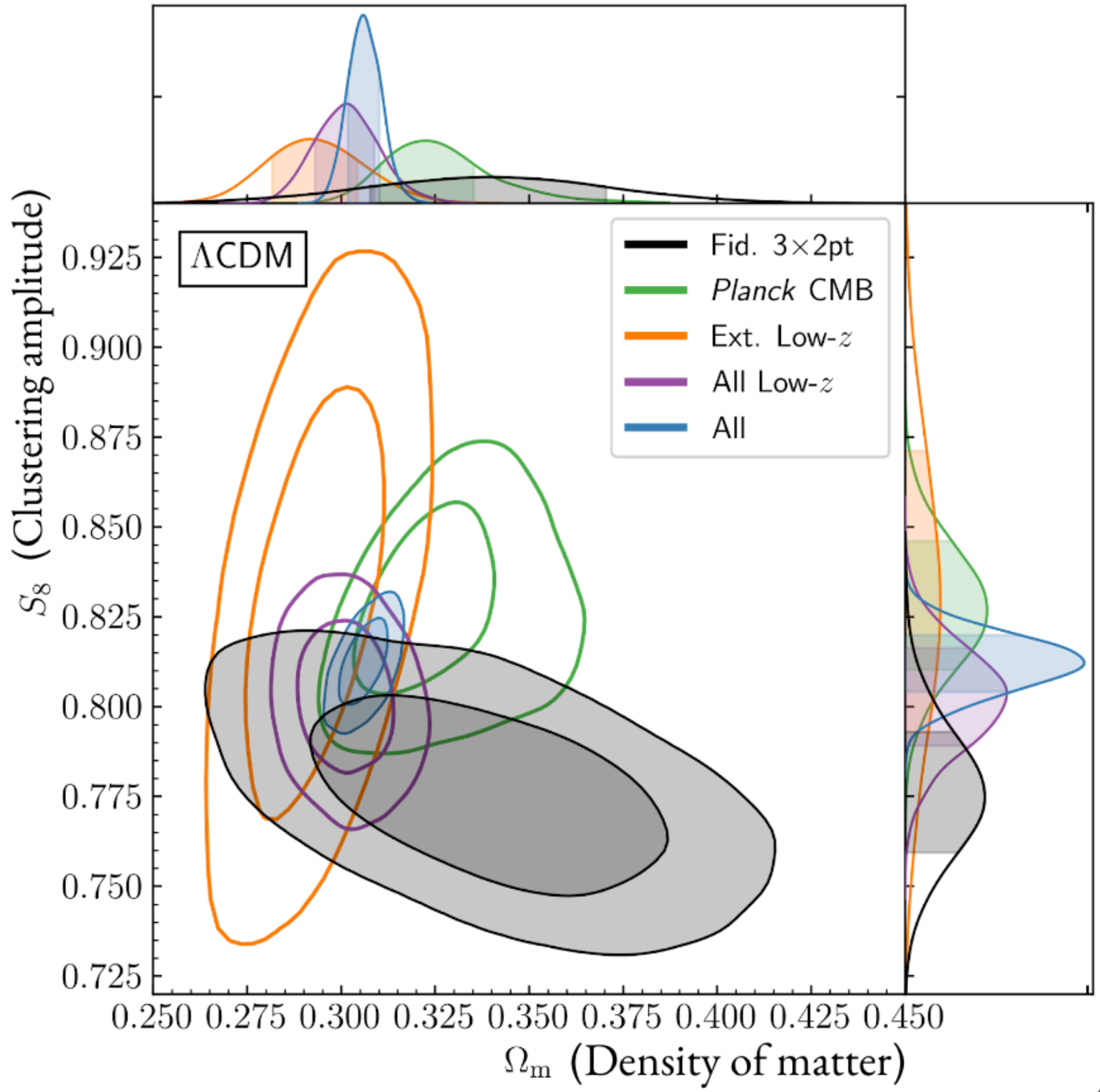

DARK ENERGY with DES 3yr

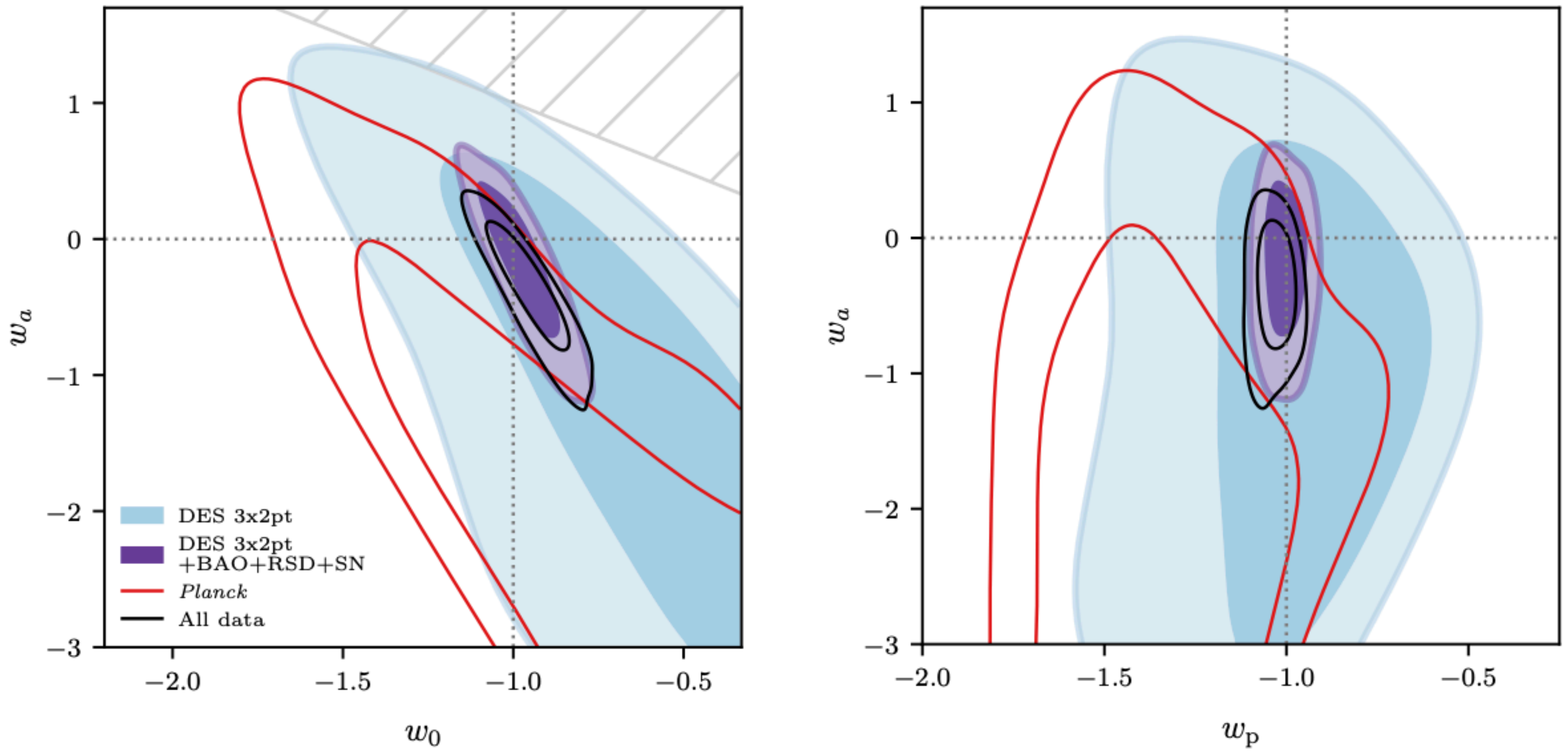

Pivot: z~0.3

arXiv:2207.05766

NEUTRINOS

STERILE NEUTRINOS

$$k_{\rm fs} = \frac{0.8h{\rm Mpc}^{-1}}{\sqrt{1+z}}\left(\frac{m_{\rm eff}}{(1{\rm eV})\Delta N_{\rm eff}}\right)$$

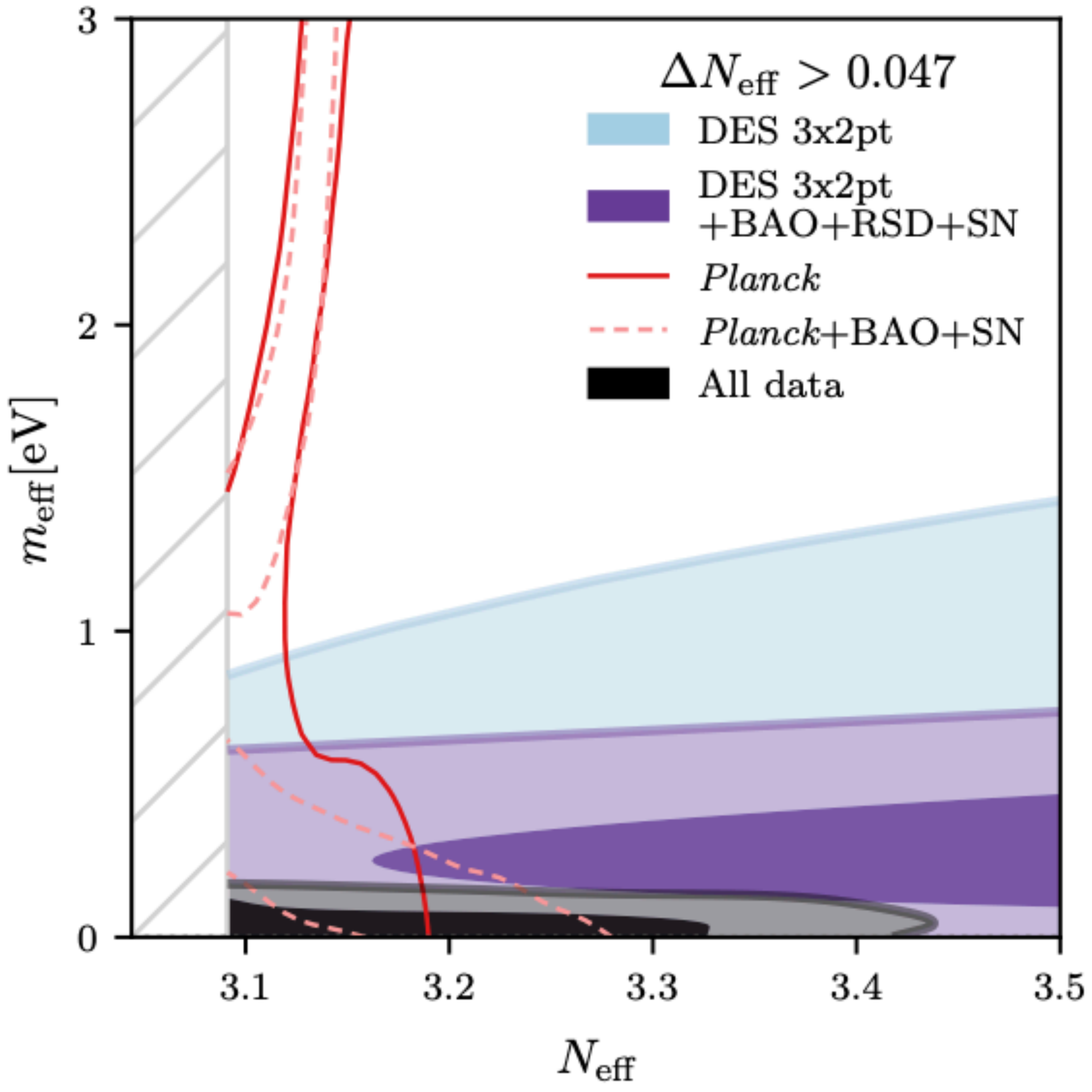

ACTIVE NEUTRINOS

	95% upper bound on $\sum m_\nu$ [eV]	
Model	All External	All data
ΛCDM	0.14	0.14
wCDM	0.17	0.19
w_0–w_a	0.25	0.26
Ω_k	0.16	0.15
$N_{\rm eff}$	0.14	0.16
Σ_0–μ_0	0.21	0.14
Binned $\sigma_8(z)$	0.30	0.20
$A_{\rm L}$	0.14	0.19

Modification of gravity and evolution of growth

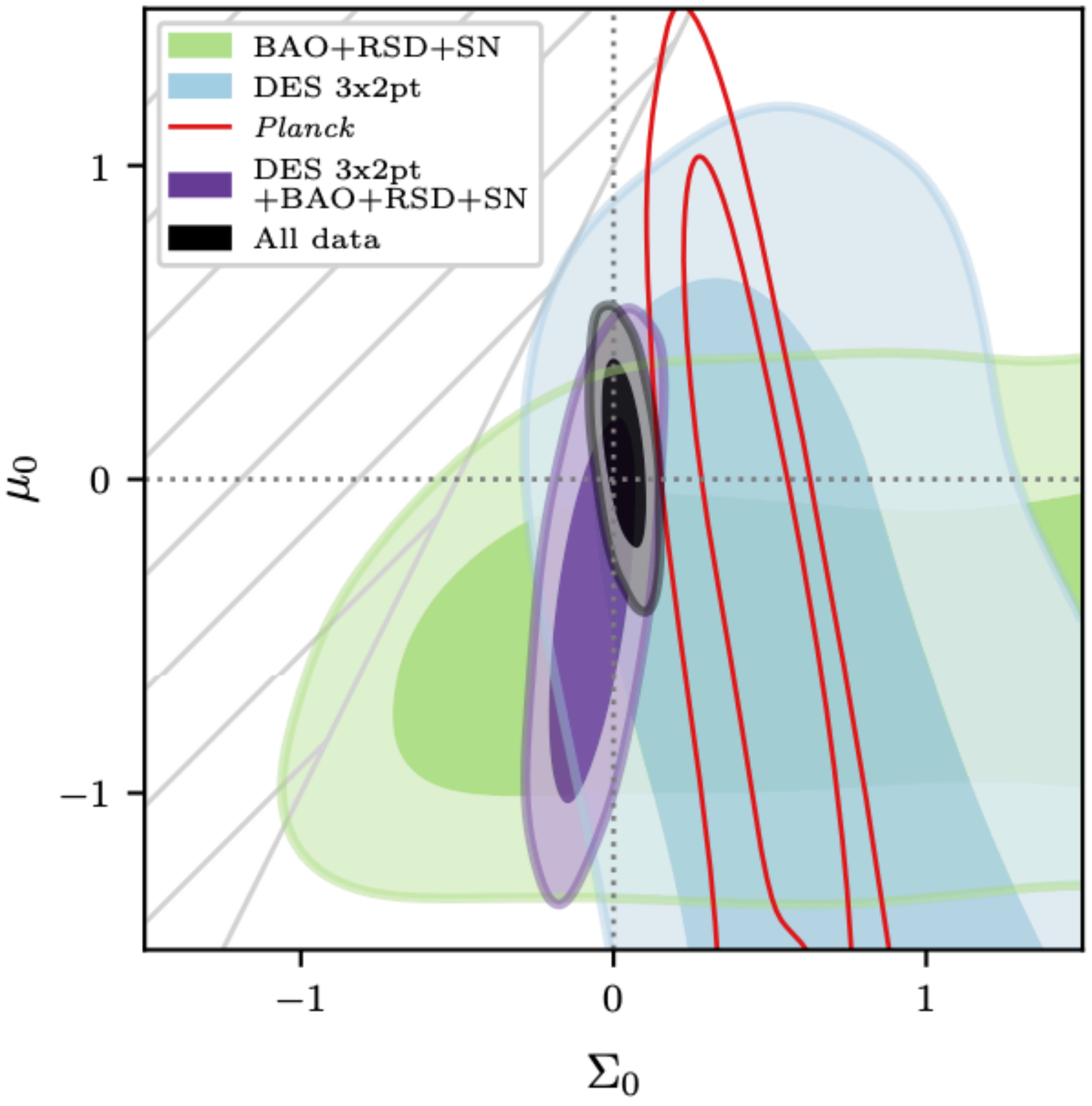

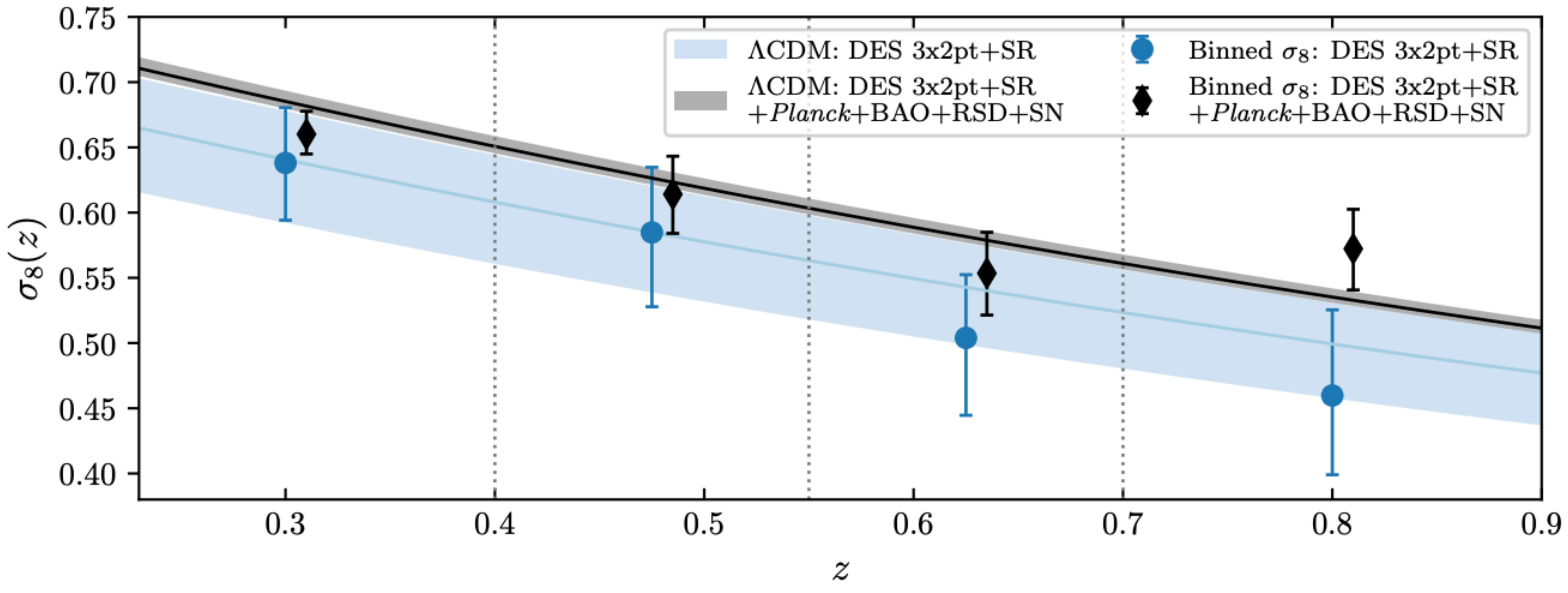

KIDS-1000

A&A 646, A140 (2021)
https://doi.org/10.1051/0004-6361/202039063

Astronomy & Astrophysics

KiDS-1000 Cosmology: Multi-probe weak gravitational lensing and spectroscopic galaxy clustering constraints

Catherine Heymans[1,2], Tilman Tröster[1], Marika Asgari[1], Chris Blake[3], Hendrik Hildebrandt[2], Benjamin Joachimi[4], Konrad Kuijken[5], Chieh-An Lin[1], Ariel G. Sánchez[6], Jan Luca van den Busch[2], Angus H. Wright[2], Alexandra Amon[7], Maciej Bilicki[8], Jelte de Jong[9], Martin Crocce[10,11], Andrej Dvornik[2], Thomas Erben[12], Maria Cristina Fortuna[5], Fedor Getman[13], Benjamin Giblin[1], Karl Glazebrook[3], Henk Hoekstra[5], Shahab Joudaki[14], Arun Kannawadi[15,5], Fabian Köhlinger[2], Chris Lidman[16], Lance Miller[14], Nicola R. Napolitano[17], David Parkinson[18], Peter Schneider[12], HuanYuan Shan[17,19], Edwin A. Valentijn[9], Gijs Verdoes Kleijn[9], and Christian Wolf[16]

Tension between WL and Planck quantified at the level of 2-3sigma

We find that the ~ 3σ tension with Planck CMB data that was found in Asgari et al. (2021) and Heymans et al. (2021) is not resolved by either extending the parameter space beyond flat ΛCDM, or by restricting it through fixing the amplitude of the primordial power spectrum to the Planck best-fit value.

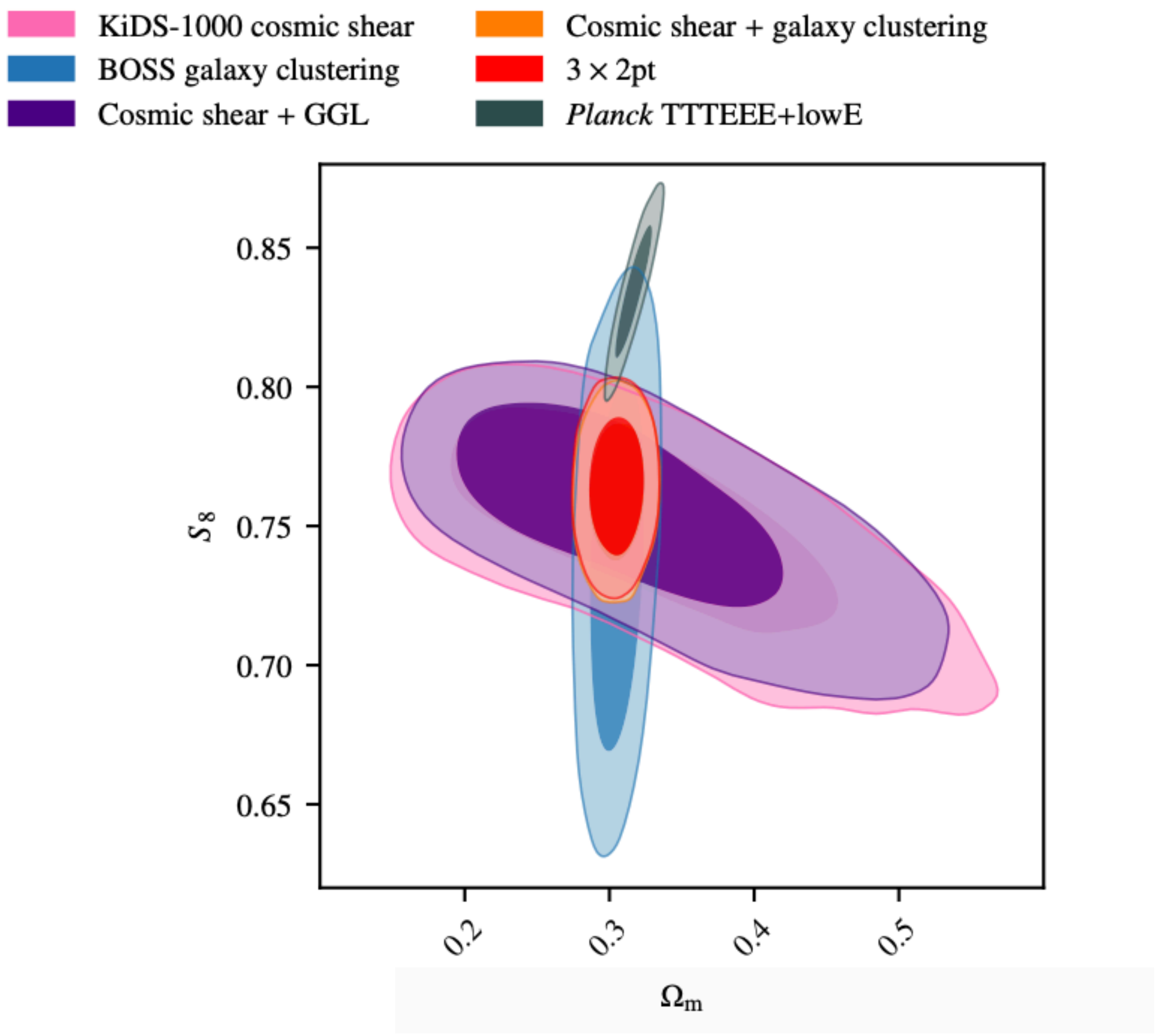

Baryonic correction model wrong???

Cosmology with Galaxy Clusters - I

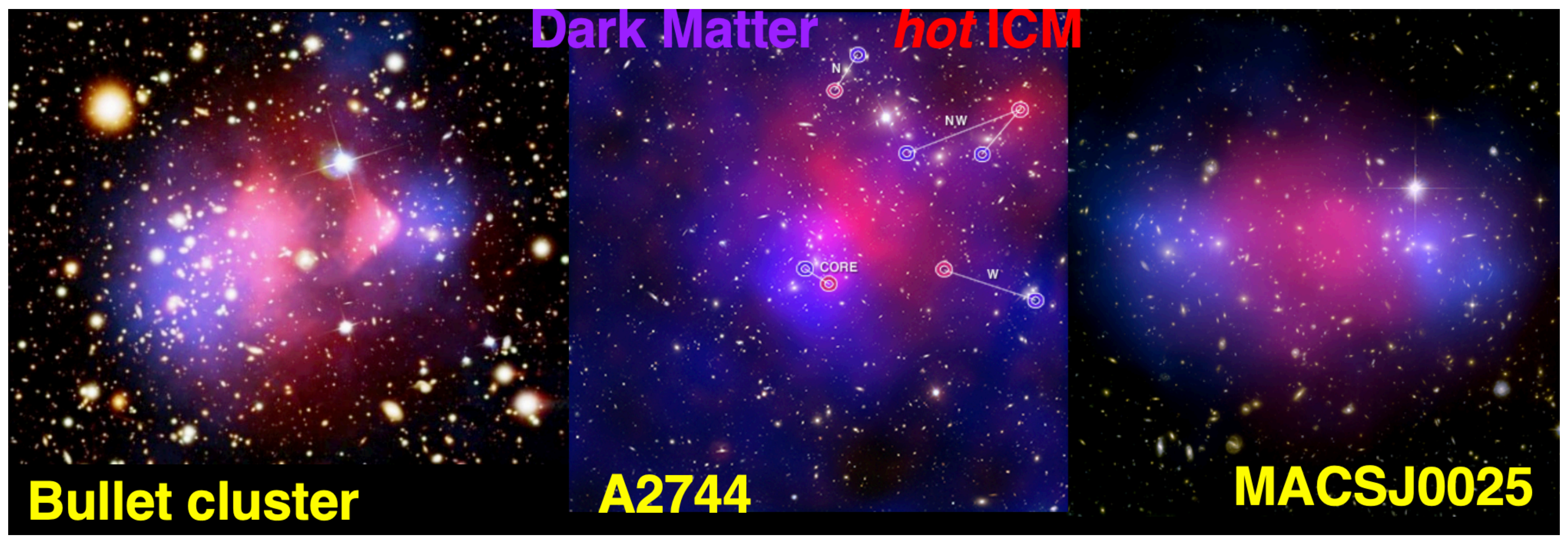

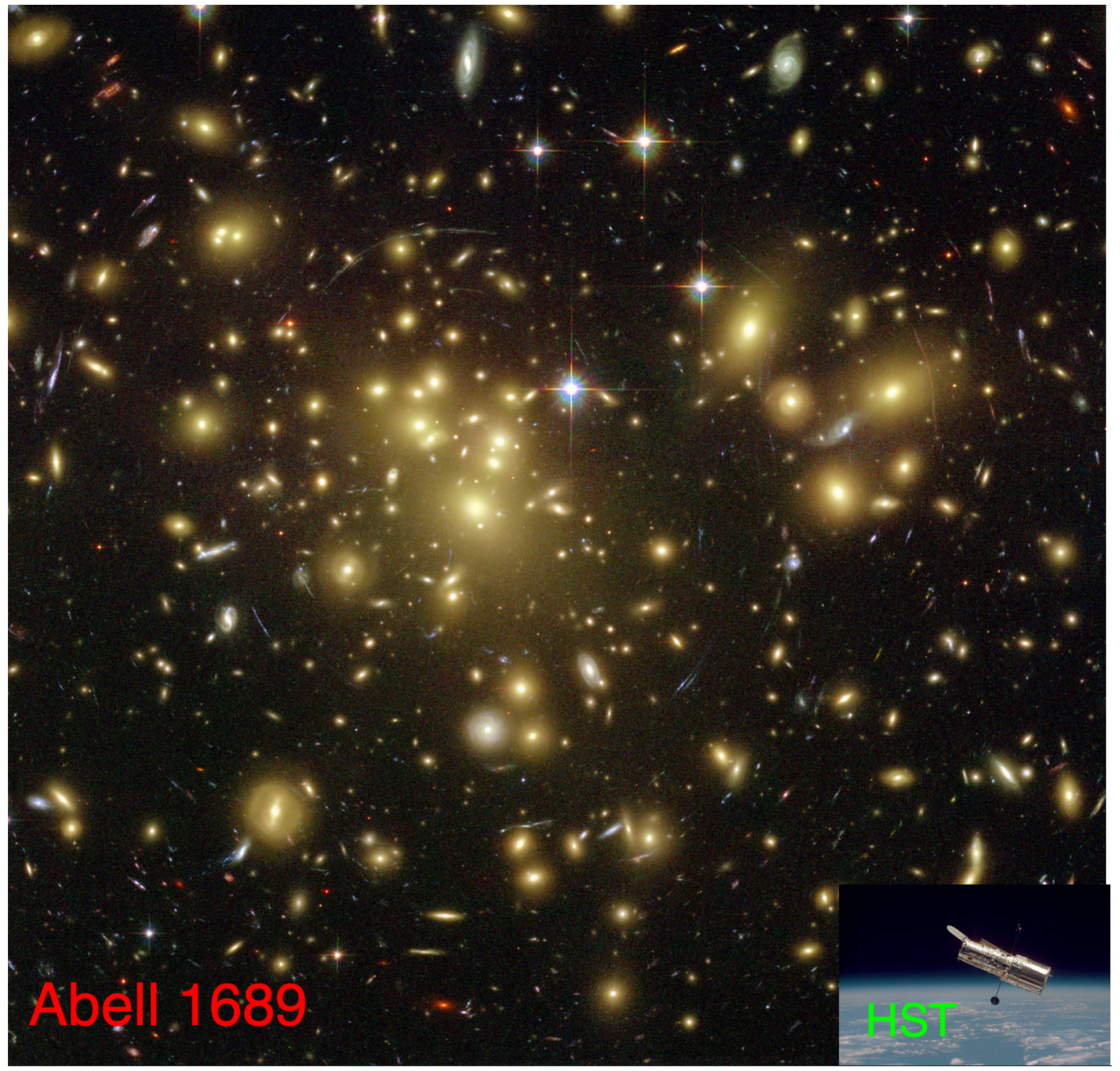

Physical properties of GCs as inferred from optical and X-ray observations

Concentrations of ~10^3 galaxies
σ_v ~500-1000 km/s
Size: ~1-2 Mpc
Mass: ~10^{14}-10^{15} Msun
➔ $\lambda_i \approx 10$ Mpc
Baryon content:
➔ cosmic share (~15%) in hydrostatic equilibrium
ICM temperature:
➔ T ~ 2-10 keV
➔ fully ionized plasma; Thermal bremsstrahlung
➔ n_e~10^{-2}-10^{-4} cm-3
➔ $L_X \sim n_e^{\,2}\, V \sim 10^{45}$ erg/s

Cosmology with Galaxy Clusters - II

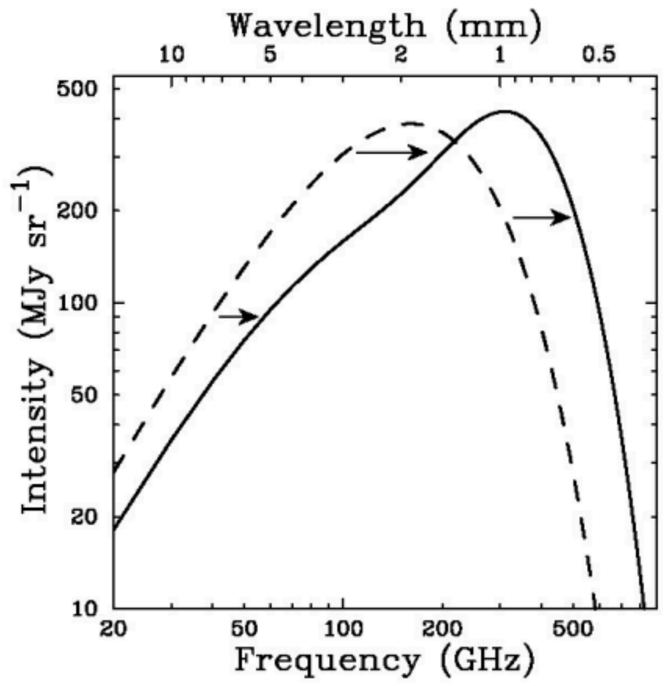

Inverse Compton scattering of CMB photons off the ICM electrons

SZ-Clusters

- ➔ Signal virtually independent of redshift
- ➔ Proportional to the l.o.s. integration of neTe ~ pressure
- ➔ Wider dynamic range accessible compared to X-rays
- ➔ We are now in the era of SZ cluster cosmology (e.g. ACT, SPT, Planck)

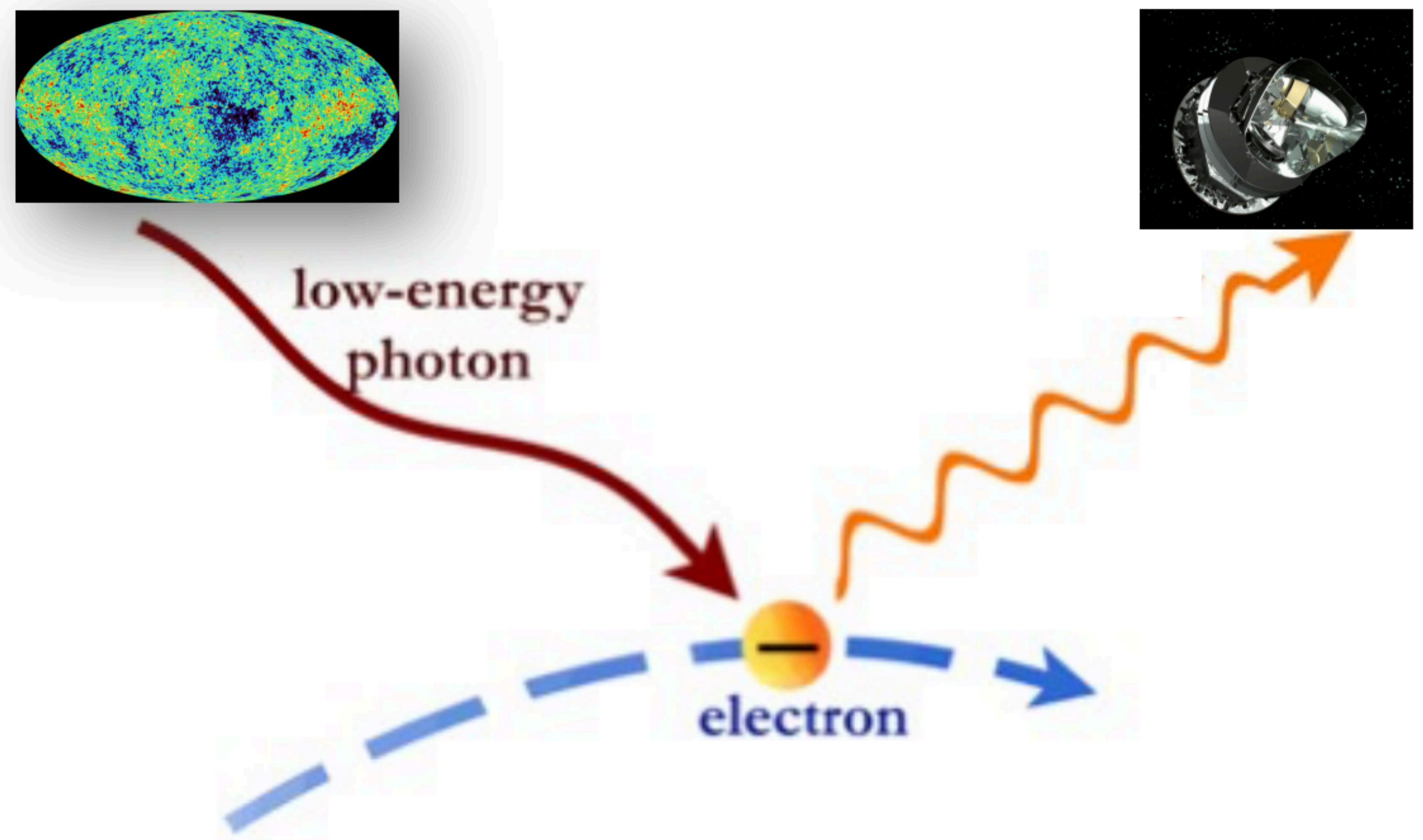

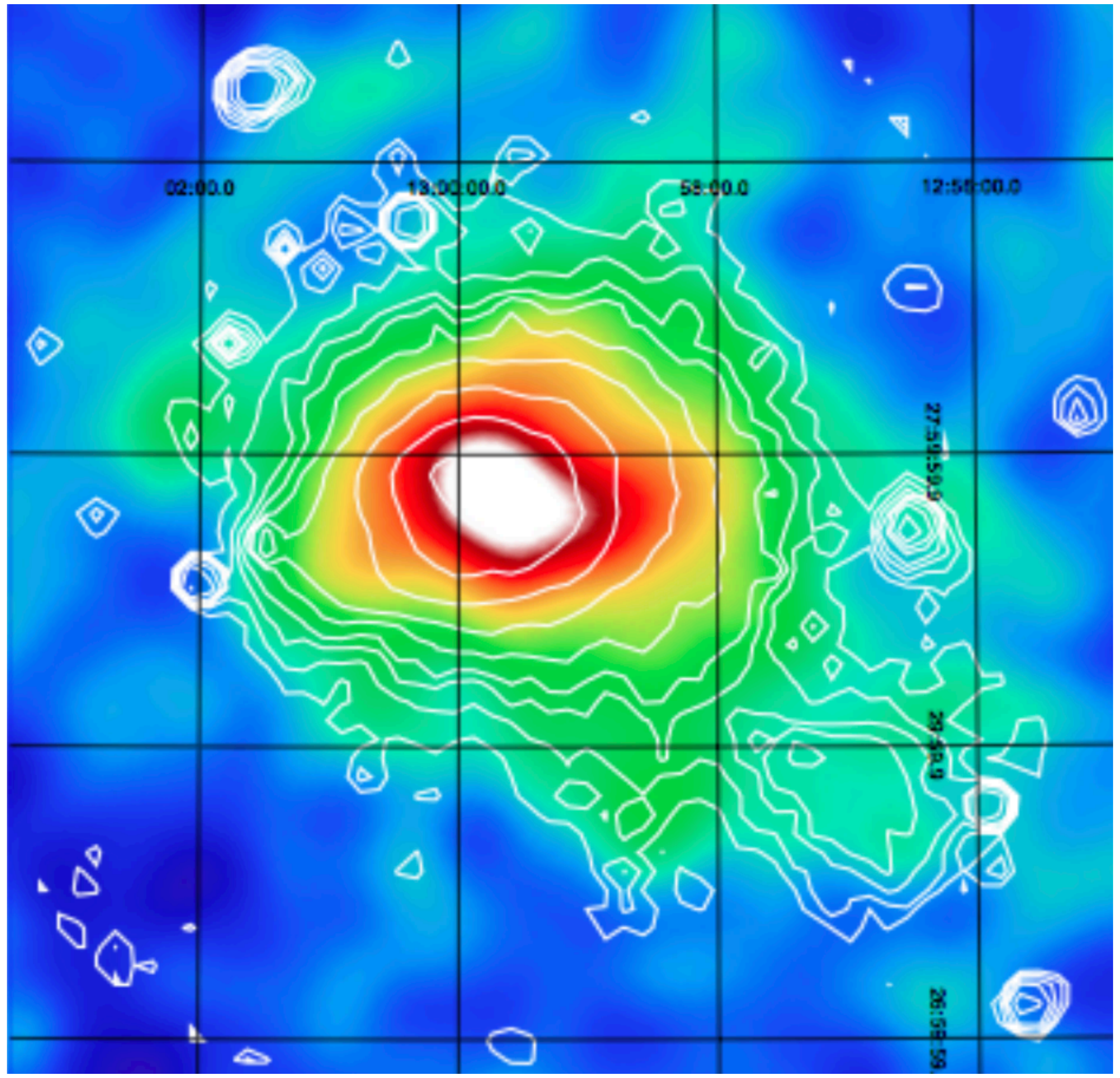

Cosmology with Galaxy Clusters - III

What do we need to do cosmology with GCs? 1) robust cluster catalogs with large z leverage (with well understood purity and completeness; look for e.g. DES, SPT-3G, eROSITA, Euclid) 2. accurate absolute mass calibration (from weak lensing or X-ray once bHE is better characterized) 3. sufficiently low-scatter mass proxy information (mainly from X-ray and SZ follow-up; optical is more expensive and still affected from large scatter)

$$\frac{dN(X;z)}{dXdz} = \frac{dV}{dz} f(X,z) \int_0^\infty \frac{dn(M,z)}{dM} \frac{dp(X|M,z)}{dX} dM$$

dV/dz: volume [priors from BAO, SN, CMB
f(X,z) observational strategy - selection function
dn/dM cosmology Mass function
dp/dX - astrophysics [from sims/mocks/observations]

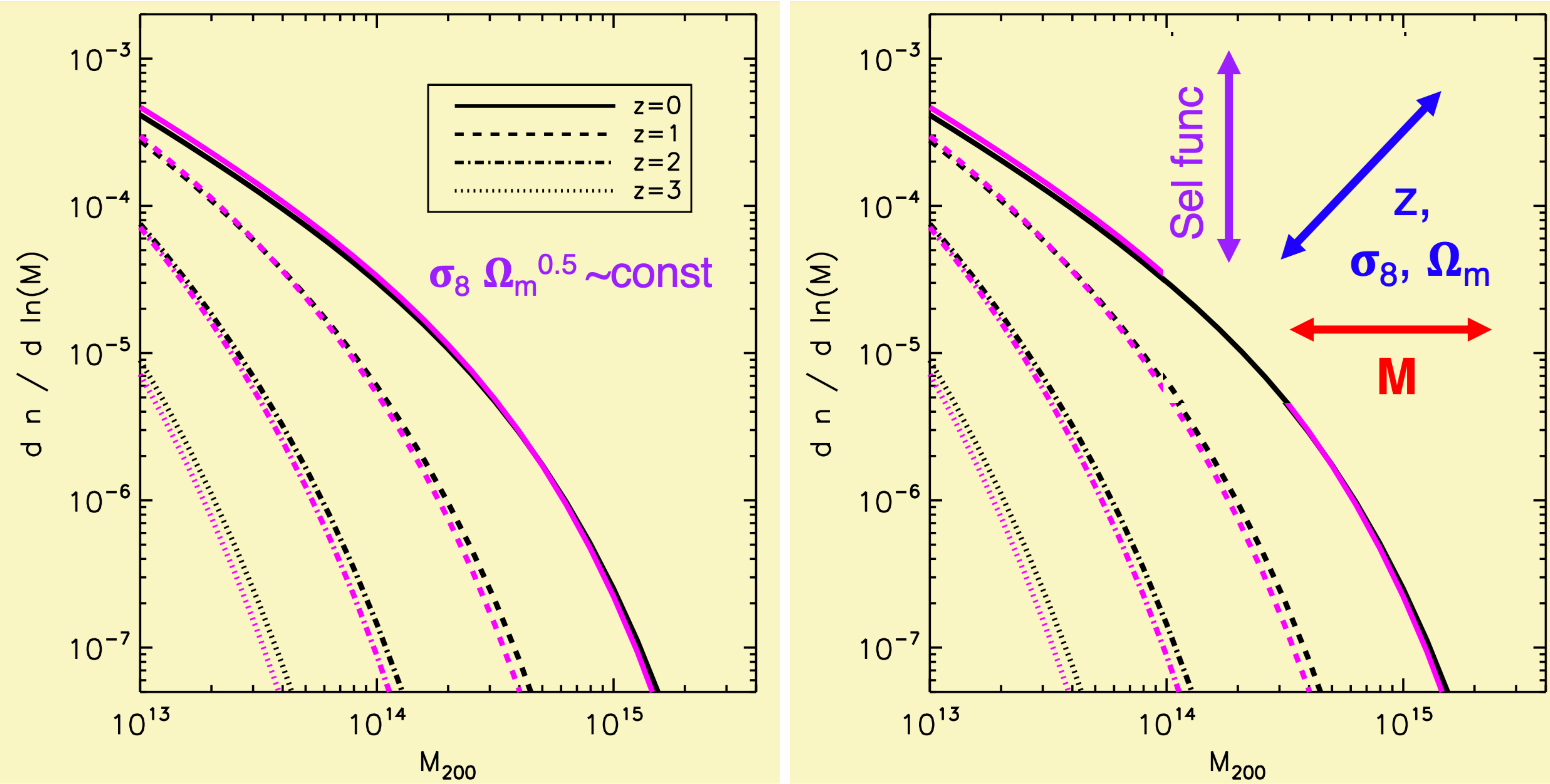

Cosmology with Galaxy Clusters - IV: constraints from gas fractions

~ 40 X-ray Clusters - measurement of f_gas
from hydrostatic equilibrium
sample of relaxed and hot GCs from Chandra
also some WL mass estimates to further constrain the model

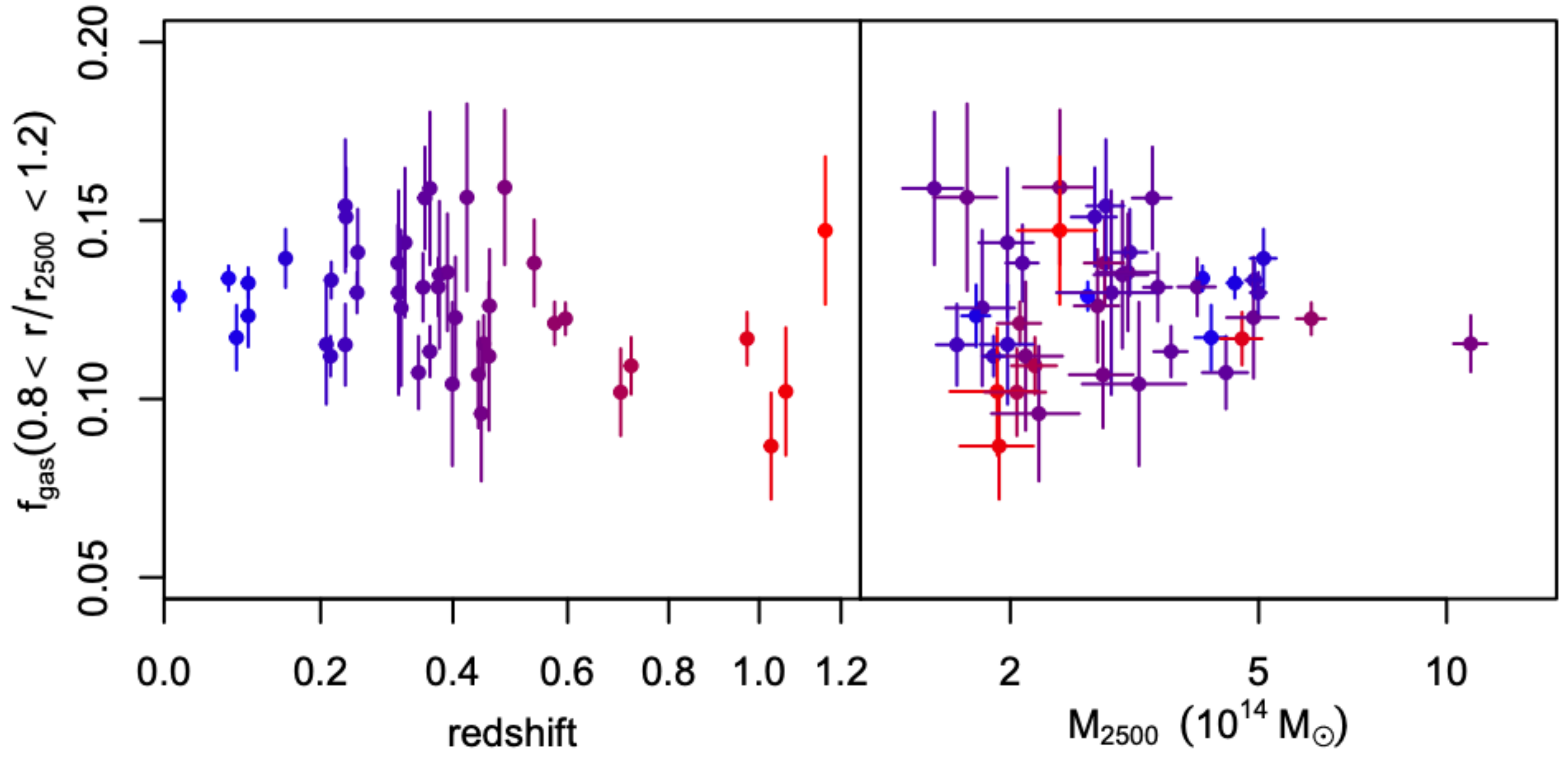

Mantz+21

$$f_{gas}(z, M_{2500}) = \Upsilon(z, M_{2500}) \frac{\Omega_b}{\Omega_m},$$

$$\Upsilon(z, M_{2500}) = \Upsilon_0(1 + \Upsilon_1 z) \left(\frac{M_{2500}}{3 \times 10^{14} M_\odot} \right)^{\alpha}$$

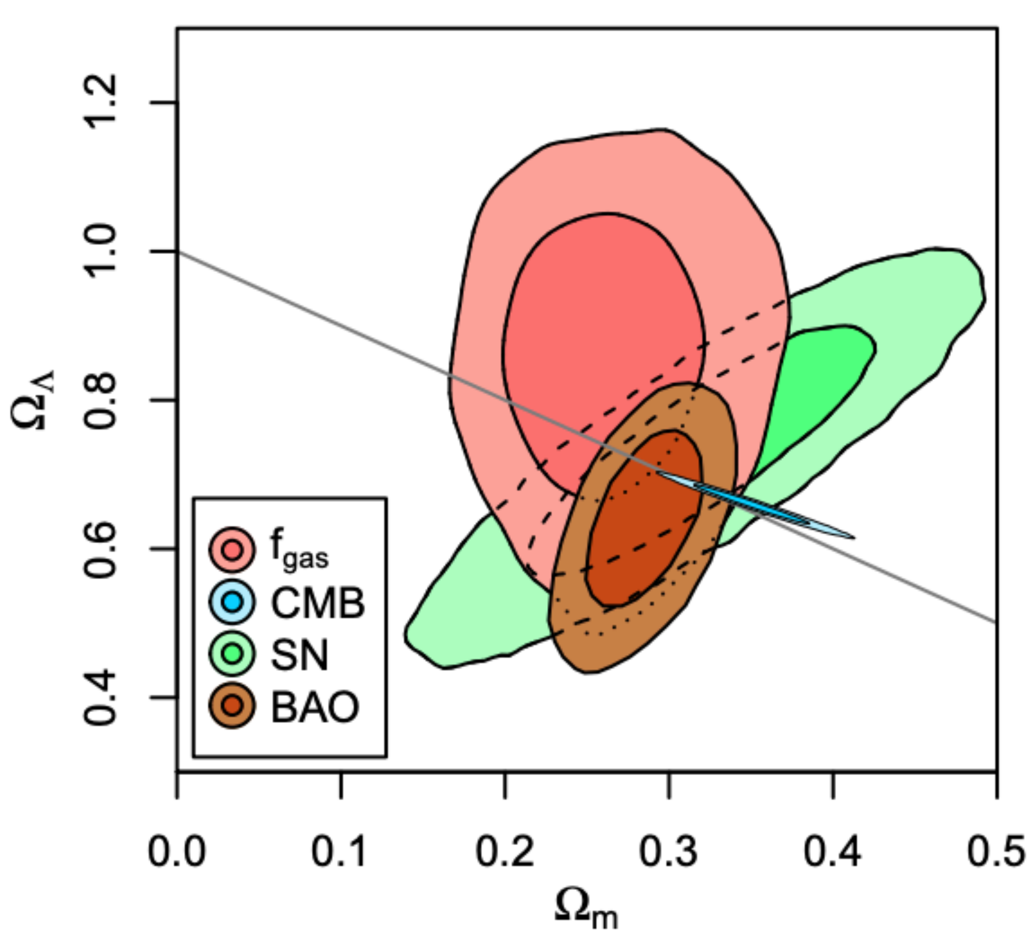

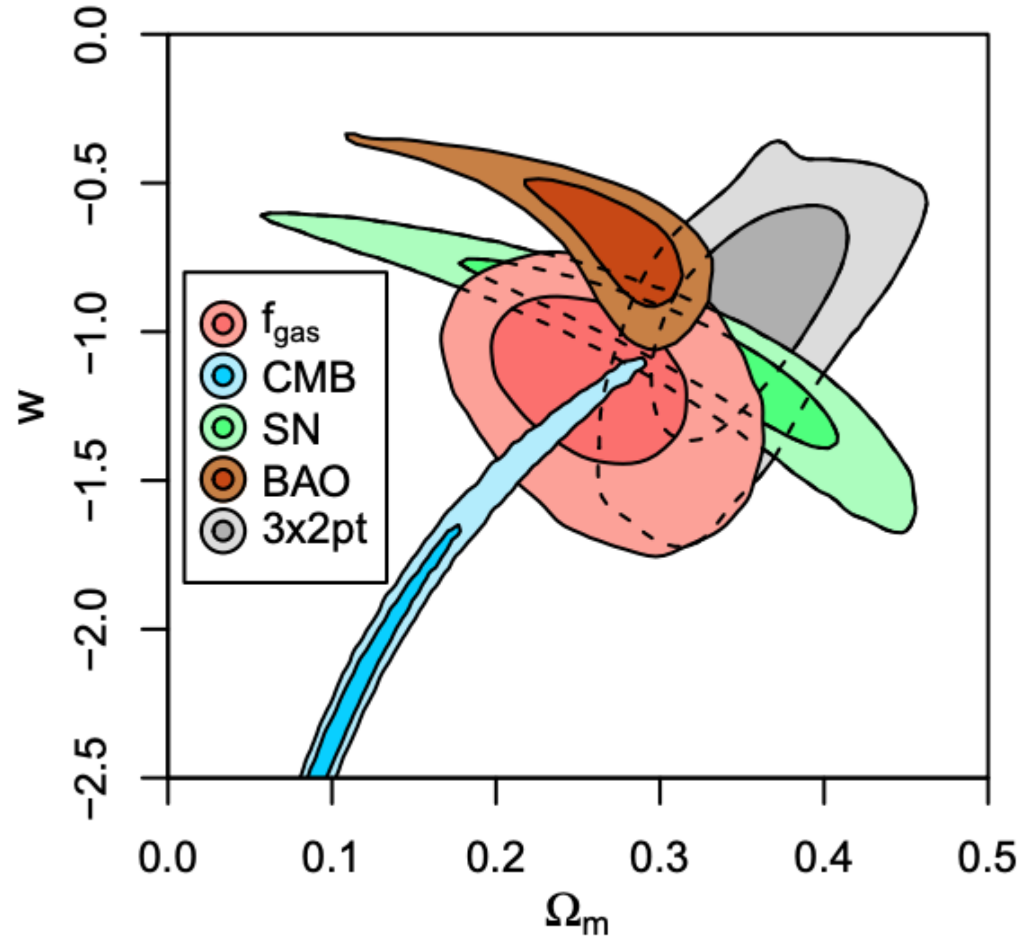

Cosmology with Galaxy Clusters - V: constraints from optical clusters

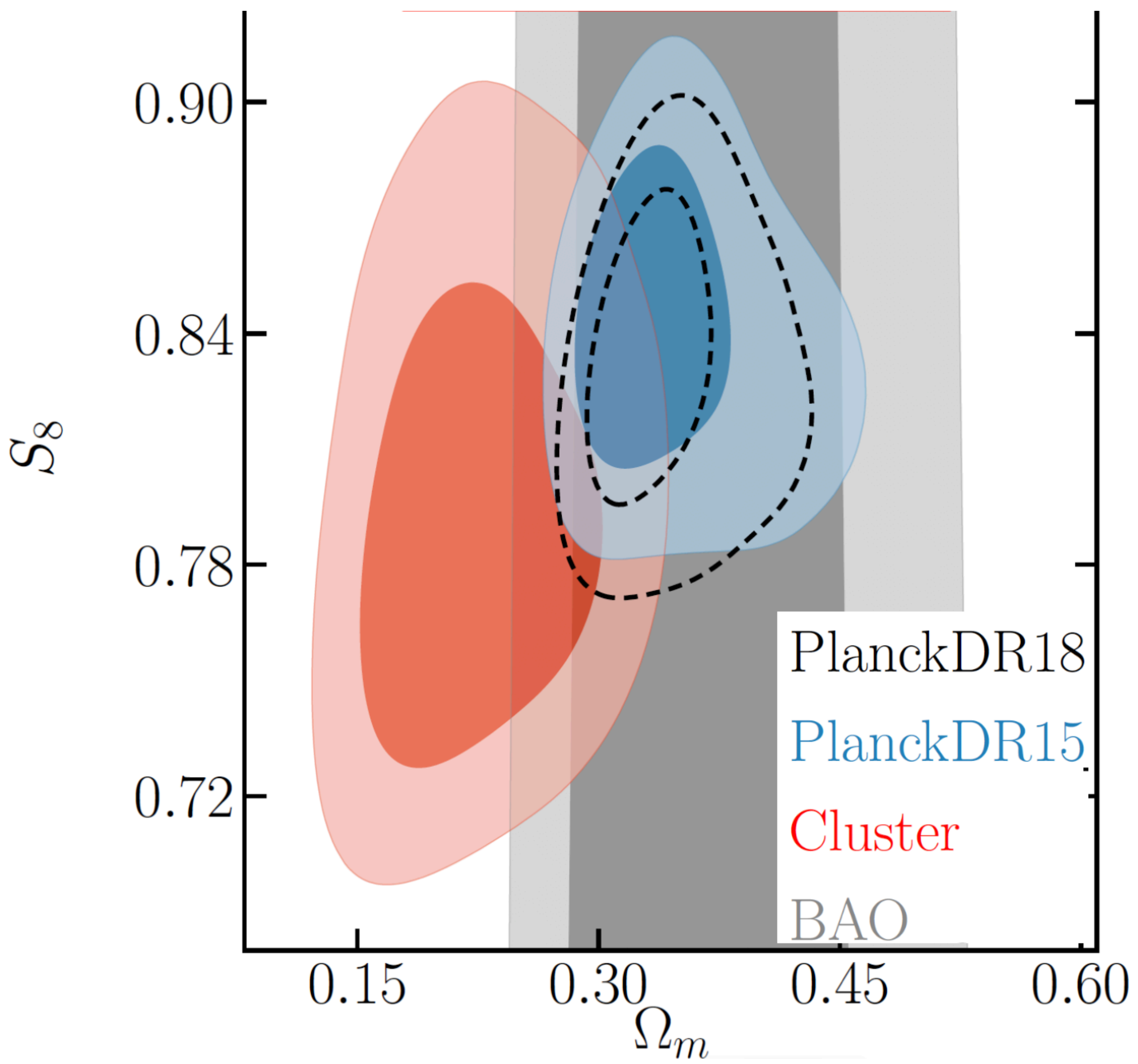

Costanzi+2018: abundance and weak-lensing of RedMapper clusters from SDSS (z=0.1-0.3)

➔ ~7000 clusters used

$$S_8 \equiv \sigma_8(\Omega_m/0.3)^{0.5} = 0.79^{+0.05}_{-0.04}.$$

No evidence of tension with CMB constraints and constraints from other cluster catalogues

Cosmology with Galaxy Clusters - VI: constraints from SZ cluster

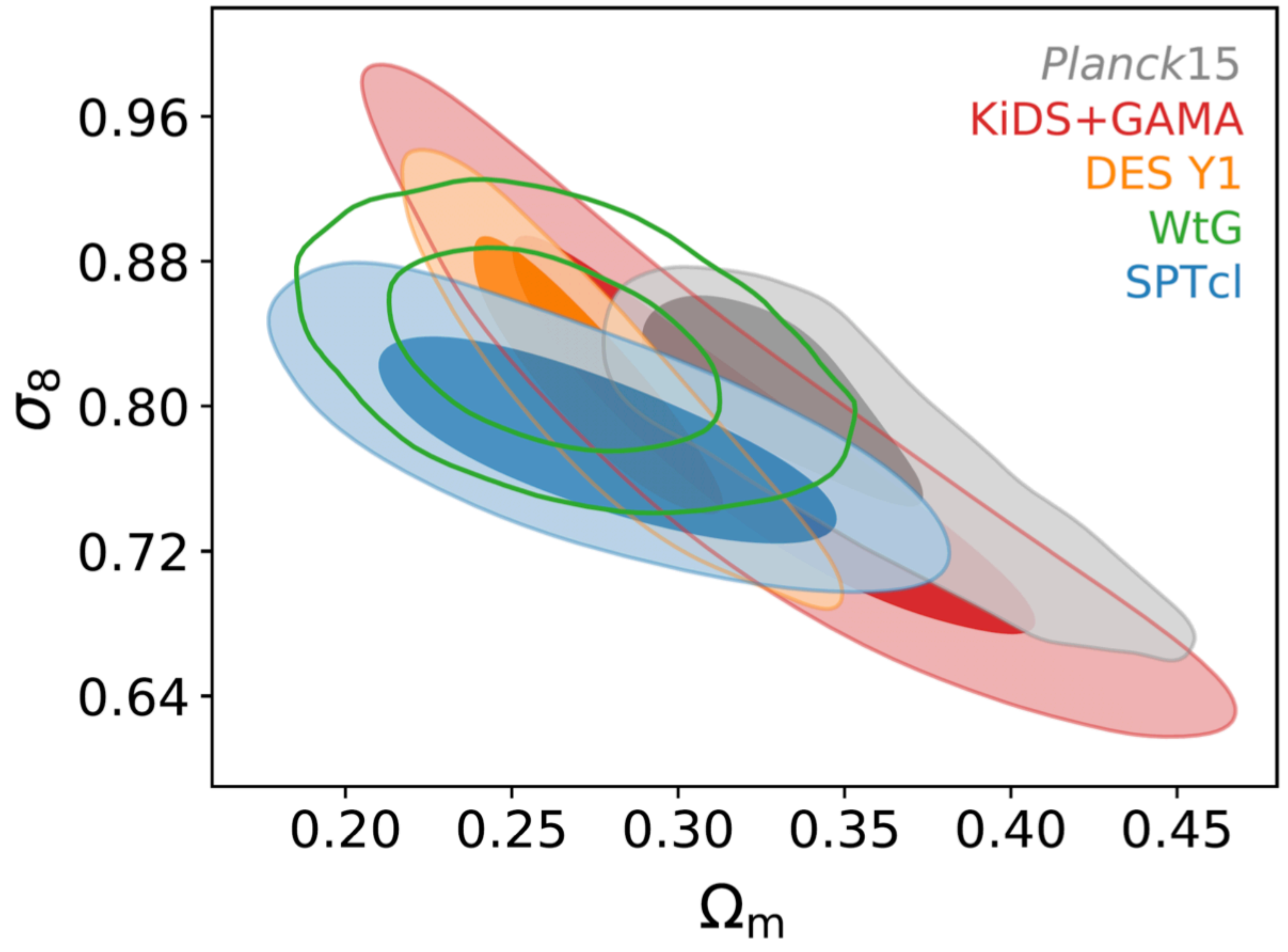

Bocquet+2018: cluster counts in the SPT-SZ survey (z=0.25-1.75)

➔ 377 clusters used, supplemented by HST+Magellan WL mass and Chandra X-ray observations

$$\Omega_m = 0.276 \pm 0.047$$
$$\sigma_8 = 0.781 \pm 0.037$$

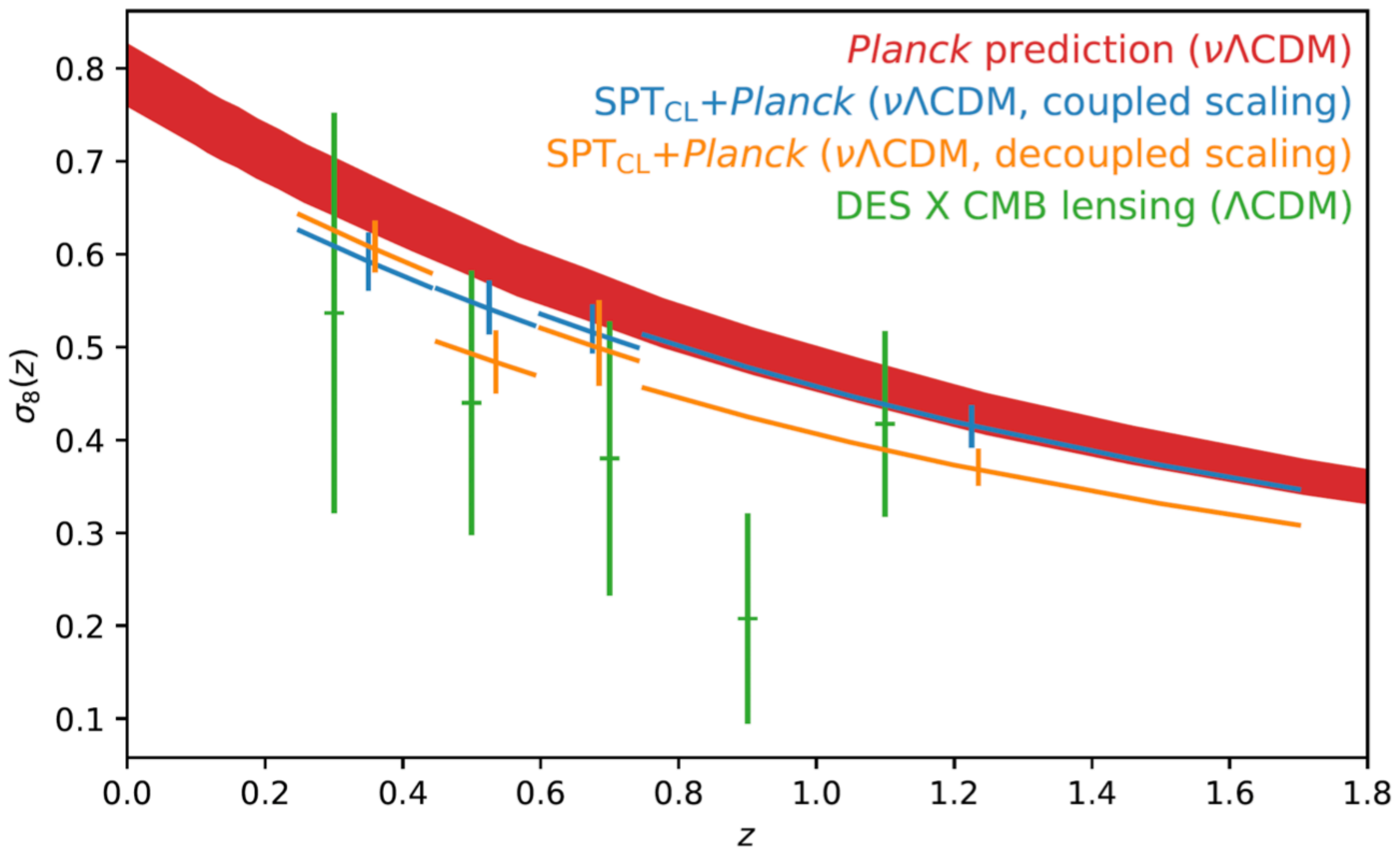

- Allow neutrino mass to be a free paramteer
- Test of growth of structure in agreement with GR

Cosmology with Galaxy Clusters

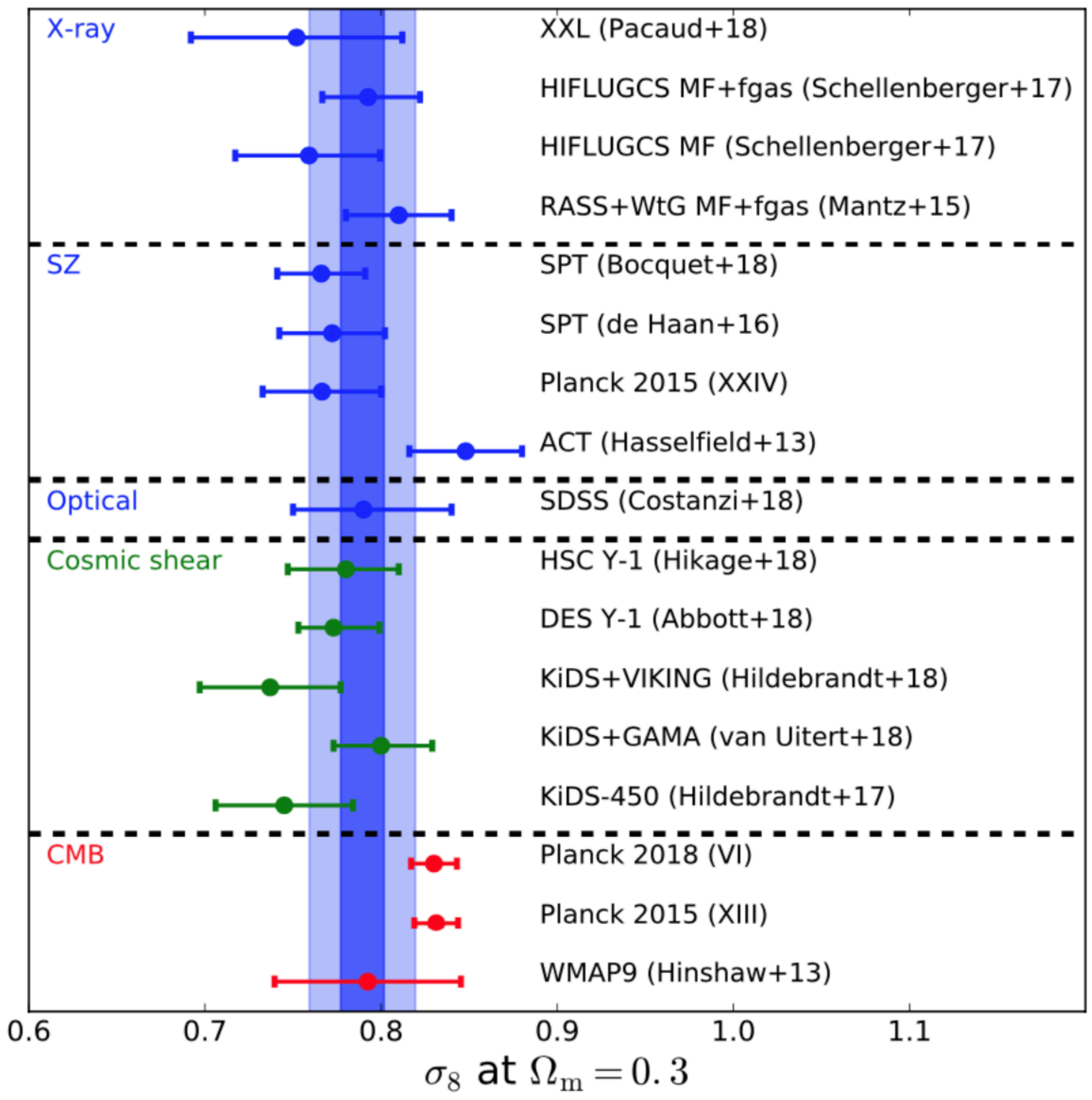

Cosmology with Galaxy Clusters and the IGM - new tension????

Esposito+22 w

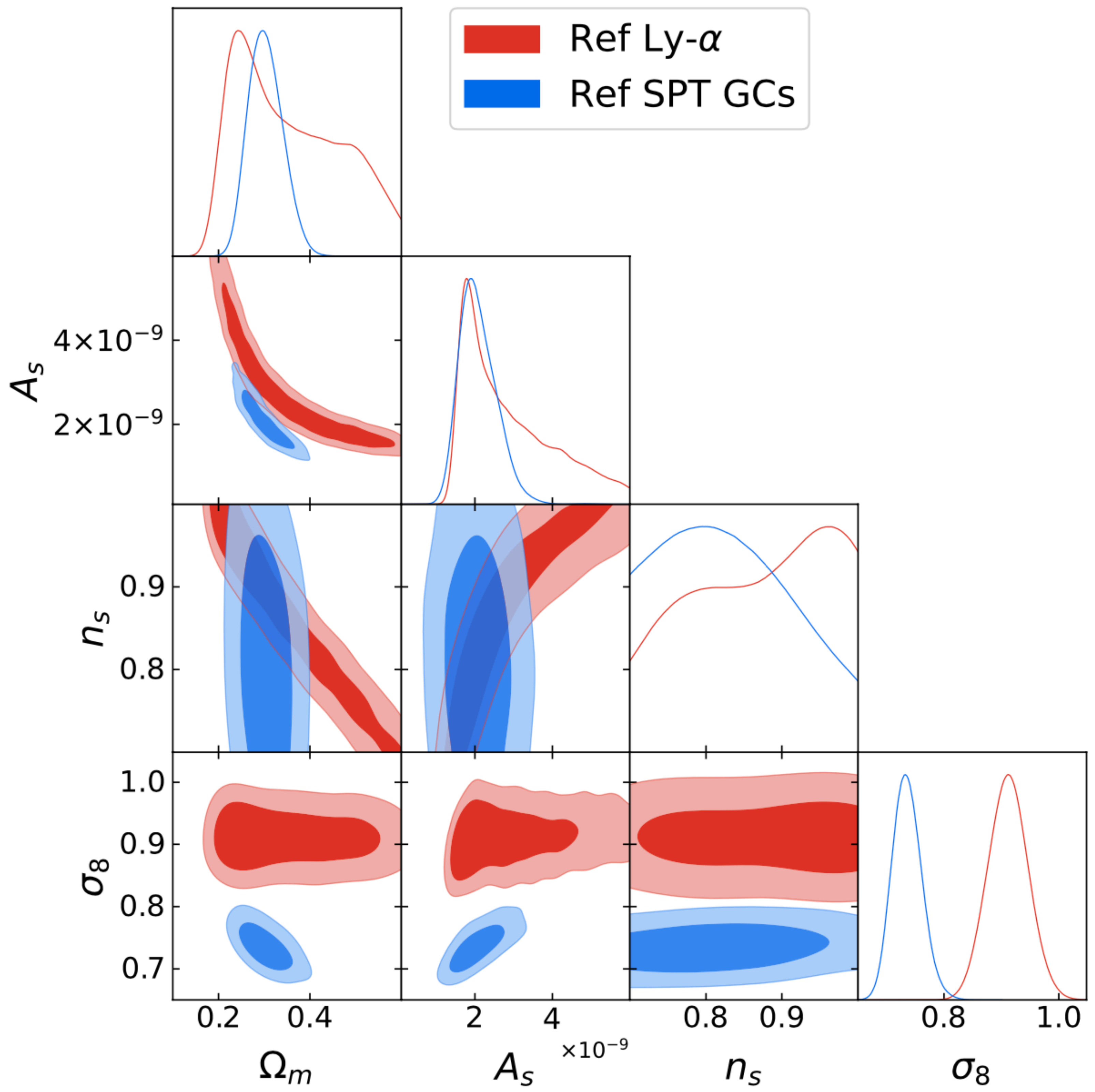

Detection signal noise-ratio vs Cluster Mass

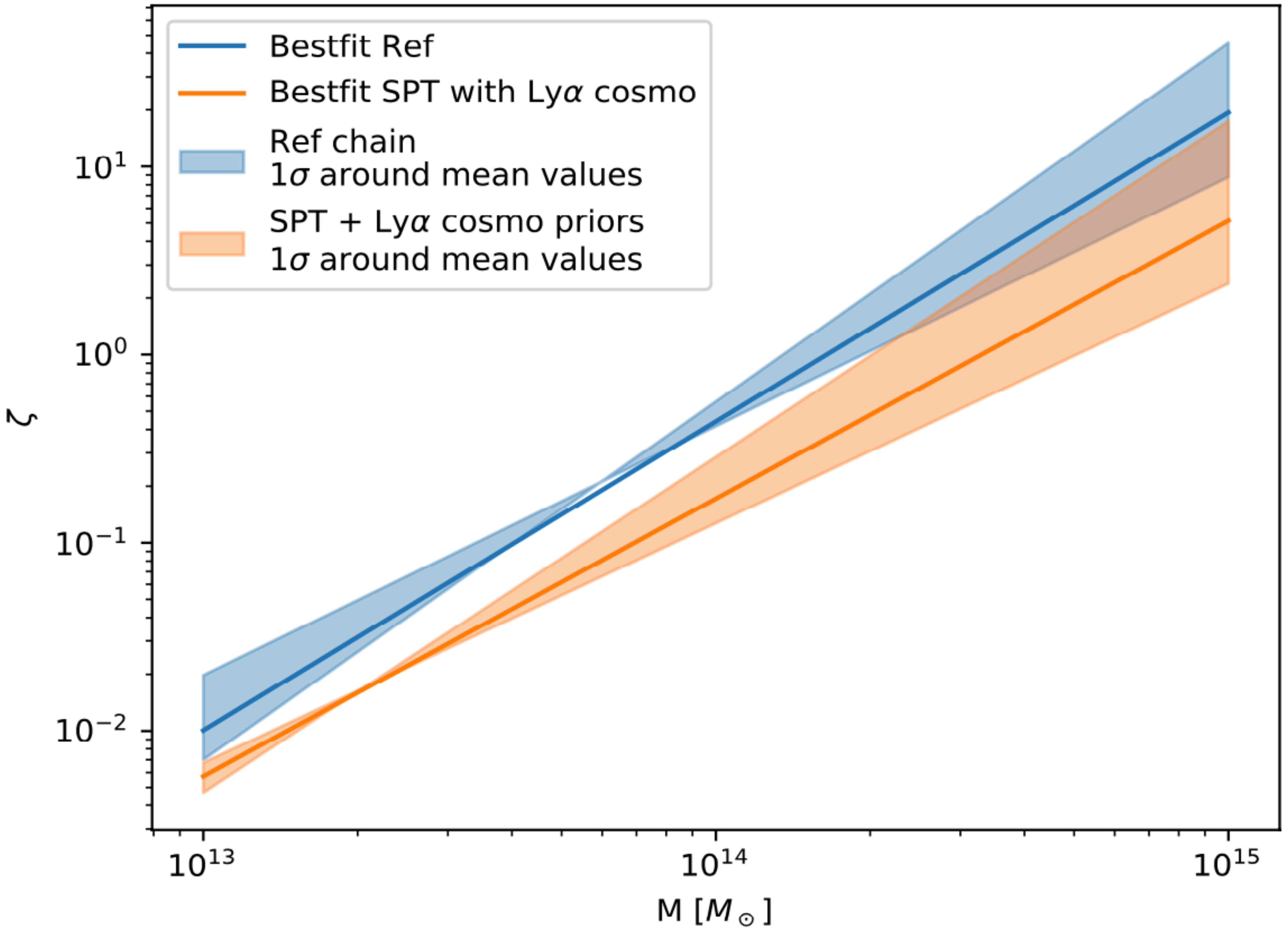

$$\langle \ln \zeta \rangle = \ln A_{SZ} + B_{SZ} \ln\left(\frac{M_{500} h_{70}}{4.3\times10^{14} M_\odot}\right) + C_{SZ} \ln\left(\frac{E(z)}{E(0.6)}\right)$$

Lensing and Clusters - Summary

- Weak gravitational lensing: fundamental cosmological observables which, unlike galaxy clustering and similarly to Lyman-alpha, allows access to non-linear scales
- Tremendous progress in the last decade: KiDS, DES, CFHTLens. Mathematically very neat modelling, in practice much harder
- Probe of structure growth: some S8 tension seems to be present
- Galaxy Cluster number counts also very important to constrain s8-Omegam: results in agreement with WL
- Again: exciting future: for WL: Euclid and LSST, for GCs: eROSITA, Euclid, Roman telescope.